DEPARTMENT OF PHYSICS
WASHINGTON STATE UNIVERSITY

ANNUAL REPORT
July, 1983

for

NASA-Ames Interchange for Joint Research
NCA2-OR840-202

FRACTO-EMISSION FROM GRAPHITE/EPOXY COMPOSITES

J. Thomas Dickinson

Department of Physics
Washington State University
Pullman, WA 99164-2814

TABLE OF CONTENTS

I. ABSTRACT

Fracto-emission (FE) is the emission of particles and photons during and following crack propagation. The types of particles we have observed include electrons (EE), positive ions (PIE), and excited and ground state neutrals (NE). In this report we present results of a number of experiments involving principally graphite/epoxy composites and Kevlar™ single fibers. A study concerned with the physical processes responsible for EE and PIE is included. Finally, a review paper on FE from fiber- and particulate-reinforced composites is also included.

II. INTRODUCTION

In this report we present four recently written manuscripts, three of which deal with the subject of fracto-emission from fibers or fiber-reinforced epoxies. The fourth paper involves recent studies on the mechanisms of electron and positive ion emission from systems where large amounts of charge separation occurs, e.g. situations involving interfacial or adhesive failure

We feel that the more details of fracto-emission mechanisms we can provide, the more useful a tool FE will be for investigating damage and failure mechanisms, the influence of environmental factors on composites, and as a sensitive probe of crack growth in composite materials.

The work presented in this report includes the following:

Section III: ACOUSTIC AND ELECTRON EMISSION FROM THE FRACTURE OF GRAPHITE/EPOXY COMPOSITES

(Submitted to J. Mater. Sci.)

Section IV: FRACTO-EMISSION FROM SINGLE FIBERS OF KEVLAR-49

(Submitted to Fibre Science Technol.)

Section V: FRACTO-EMISSION: THE ROLE OF CHARGE SEPARATION

(Submitted to J. Vac. Sci. Technol.)

Section VI: FRACTO-EMISSION FROM FIBER- AND PARTICULATE-REINFORCED COMPOSITES

(A review paper which will be published in the Proceedings of the Symposium on Polymer Composites-Interfaces, Plenum Press (1983))

III. ACOUSTIC AND ELECTRON EMISSION FROM THE FRACTURE OF GRAPHITE/EPOXY COMPOSITES

A. Jahan-Latibari, J. T. Dickinson, and L. C. Jensen
Department of Physics
Washington State University
Pullman, WA 99164-2814

ABSTRACT

The failure mechanisms of graphite-epoxy composites are investigated using acoustic emission (AE) and electron emission (EE) techniques. EE and positive ion emission (PIE) from the fracture of unidirectional graphite-epoxy composites were measured. The results show a rapid rise in emission during fracture and a slow decay following fracture for both EE and PIE. Multidirectional graphite-epoxy composites fractured in flex were examined as well. The simultaneous AE and EE measurements indicated a steady build-up of AE prior to catastrophic failure in all systems examined. A slow, pre-fracture EE build-up was detected from the flexural loading of zero degree graphite-epoxy. This was attributed to microcrack formation in the matrix as well as the separation of the tiny bundles of fibers from one another on the tension side of the sample. The steady build-up in AE was considered to be the result of fiber fracture and interlaminar failure. The results of this study suggest that by comparing data from AE and EE techniques, one can detect and differentiate between the onset of internal and external failure in composites.

I. INTRODUCTION

In acquiring an understanding of the performance of composite structures, it is essential to accurately describe the processes leading up to crack formation in model composites under stress. To gain this understanding, a number of techniques have been developed for sensing damage to these materials prior to failure. Acoustic emission (AE) is an example of such a technique; it has been used successfully to detect areas of weakness in composite specimens prior to failure (1,2). Bailey, et al. were able (3), with the aid of AE, to detect the location of flaws within composite components and investigate the time-dependent formation and propagation of cracks during loading. Rotem (4) was able to discriminate between different failure modes in composites by analyzing amplitude intensity distributions of AE.

In recent months we have been investigating a set of physical phenomena called fracto-emission (FE) that involves the emission of particles (e.g. electrons, positive ions, neutral molecules, and photons) during and following the propagation of a crack. Most of our work has concentrated on electron emission (EE) and positive ion emission (PIE), which have been detected from a wide range of materials (see references 5 - 17). The results from the fracture of individual 10 μm fibers of E-glass, S-glass, and graphite (11,17) showed the emission from these materials to be relatively intense (typically 10^8 particles per cm^2 of cross-sectional area) and short-lived, typically decaying away in 10 - 50 μs. The fracture of Kevlar™ fibers (18) produced multiple bursts of emission, indicating the formation and fracture of individual fibrils within the strands. These bursts, approximately 50 μs in duration, were often hundreds of microseconds apart in groups of 1 - 5.

Unfilled epoxy (DER 332/T403, a bisphenol-type A resin) yielded relatively weak emission (typically 10^3 particles per cm^2 of cross-sectional area) with a decay time of about 25 us.

Fracture of the filament/epoxy strands resulted in significantly different emission curves. During fracture, the EE and PIE rise together in the form of large bursts. Immediately following separation this intense emission begins to decay away; the decay is very slow and lasts for many seconds. Intense emitters can yield detectable emission for as long as two hours after fracture. As discussed elsewhere (11 - 16) we have found this behavior to be characteristic of interfacial or adhesive failure. A model involving the physical phenomena accompanying such fracture is presented in reference 19, wherein the charge separation between dissimilar materials in contact (e.g. epoxy/glass) plays a critical role.

In this paper the results of EE and PIE measurements from the fracture of unidirectional graphite-epoxy composites are presented; a study of multi-directional graphite-epoxy, including a comparison of AE and EE from flexural loading of such composites, is also included.

II. EXPERIMENTAL PROCEDURE

Unidirectional graphite-epoxy composites (provided by NASA-Ames Material Science and Application Office) made from Union Carbide Thornel 300 graphite fibers and NARMCO 5208 epoxy resin were fractured in tension. A sharp notch was made in the center of the tension sample to control the fracture initiation. Graphite-epoxy composites made from Union-Carbide Thornel 300 fibers and various NARMCO epoxy resins were tested in flex as well. The fiber directions in these composites were (0), ($^{+}$45) and (0,90,90,0) degrees to

the long axis. Samples were tested in three-point flex with a span-to-depth ratio of 30:1 and strain rate of 0.064 mm/sec.

The experiments were performed in a vacuum chamber at a pressure of $1x10^{-5}$ Pa. The detectors used for charged particles are channeltron electron multipliers (CEM's) which produce fast (10 ns) pulses with approximately 90% absolute detection efficiency for electrons and nearly 100% efficiency for positive ions. The gains of the CEM's used were typically 10^6 - 10^8 electrons/incident particle. The detectors were positioned 1 - 4 cm away from the sample with a bias voltage on the front cone of the CEM to attract the charged particles of interest. Background noise counts ranged from 1 to 10 counts/second. Standard nuclear physics data aquisition techniques were employed to count and store pulses, normally as functions of time. The time scales of interest are submicrosecond to several second intervals, which we can easily cover with commercial electronics.

Acoustic emission (AE) and EE were detected from graphite-epoxy composites fractured in three-point flex. AE was detected with a PZT transducer with a resonant frequency of 175 KHz. The bursts were typically 500 μs in duration. The filtered and amplified signal was fed into a discriminator to eliminate background noise, and the resulting pulses were counted on a multi-channel scaler. Thus the count rate displayed is determined by both the number and size of AE bursts (the number of "rings" that trigger the discriminator). To reduce the influence of mechanical AE in our experiments the mechanical supports were covered with teflon tape. Fracture of a uniform material (PMMA), which will have no interlaminar shear or delamination, shows no prefracture AE in our system. Fig. 1 shows schematically the electron multipler and AE transducer arrangement which simultaneously detects AE and EE from the sample. Load and deflection were also measured.

III. RESULTS AND DISCUSSION

The results of EE and PIE from the fracture of unidirectional graphite-epoxy composite (Thornel 300/5208) are shown in Fig. 2. The samples were 0.25 mm thick and 2.4 mm wide. In general EE exceeds PIE in terms of total emission by 10-40%. However, since the EE and PIE shown in Fig. 2 were measured from two separate samples, a larger variation is present between EE and PIE. The resulting emission plotted on a log scale shows the rapid rise during fracture and slow decay following fracture. We note that the decay kinetics for both EE and PIE are essentially identical, suggesting that a common rate-limiting step is shared by the two types of emissions.

Examinations of the fracture surfaces on a number of systems involving adhesive failure or delamination with an SEM indicate that the production of interfaces is responsible for intense emission during and slow decay following fracture. This feature of intense, long-lasting emission may serve as a measure of the extent of delamination that has occured. By far the majority of the emission is coming from the surfaces created by the separation of the filaments from the matrix. Even though emission accompanying composite fracture (interfacial failure) is more intense and lasts longer than emission from single fibers, the intensity at fracture and decay rates vary among various composite systems. Emission from graphite-epoxy samples decays to the background level after about 60 seconds (see Fig. 2), while emission from Kevlar-epoxy strands lasts as long as two hours. SEM observations showed interfacial failure in both composite systems, but the interfacial fracture energy may be the cause of the variations in emission decay rates.

Graphite-epoxy composite is brittle and fractures with less energy than a tougher composite system such as Kevlar-epoxy.

To further explore the type of fracture events in composites which lead to FE, we simultaneously examined the AE and EE accompanying flexural failure. Figs. 3 thru 6 show the results of AE and EE measurement from NARMCO 5208 epoxy resin and $(0)_{16}$, $(\pm 45)_{16}$, and $(0,90,90,0)_{16}$ degree graphite-epoxy composites. Load vs. deflection curves are also included in figures 4 thru 6 to better demonstrate the dependence of AE and EE on the deformation and failure of composite materials. Samples tested in flex contained no notch. Flexural testing of NARMCO 5208 epoxy resin produced a few low intensity AE bursts prior to fracture, but no EE was detected. The single bursts of AE prior to fracture are assumed to be the result of microcracking. The AE and EE count rate at fracture for epoxy resin is one order of magnitude smaller than graphite-epoxy composites. The AE data obtained from the flexural testing of graphite-epoxy composites can be characterized as follows: first, an initial rapid rise from zero due to the initial load applied to the specimen; second, the steady build-up of the AE count rate prior to failure. Finally, a large burst followed by a drop in AE count rate at catastrophic failure.

Concerning AE only, our results differ somewhat from those of Barnly and Parry (20). Barnly and Parry observed no acoustic activity prior to fracture for unidirectional fiber glass-epoxy composite notched samples tested in flex. In their experiment, the onset of failure and large load drop was indicated by the onset of AE. However, their result on cross-ply (0/90) material showed the AE build up immediately following the application of load. Fitz-Randolph et.al. (21) have shown the steady increase of AE with deflection for unidirectional boron-epoxy composites. This was expected because brittle composites such as graphite-epoxy produce different forms of AE bursts than

glass-epoxy composites.

Composite materials generally exhibit a variety of failure modes, including matrix cracking, debonding, fiber breakage resulting from statistical distribution of fiber strength, delamination, and void growth (22). Some of these events, prior to failure, will be clearly detectable in both EE and AE.

The basic requirement for detecting fracture events with EE is that the newly created fracture surfaces are in some manner in communication with the vacuum so that the particles can escape from the sample and be detected. Thus, the existence or lack of correlations between AE and EE can provide information on the mechanisms leading up to failure.

For example, Fig. 5 shows the AE build-up from a $(0)_{16}$ degree graphite/epoxy system at the early stages of loading. As mentioned previously, a statistical distribution of strength exists among graphite fibers; therefore some fracture at a lower stress in tension than others, which will produce bursts of AE. As the loading advances more fibers fracture and cause the AE build-up prior to catastrophic failure of the composite (23). Shear and internal delamination will also contribute to AE. Loose fibers at the edges may break at any time during loading and produce both AE and EE bursts simultaneously. The failure of fiber bundles are shown by two large EE and AE bursts early in loading in Fig. 5. These failures were also observed with a video recorder and correlated with the AE and EE. At higher load levels, fiber fracture and internal delamination will lead to AE. Matrix cracking in the tension side of the sample and the separation of tiny bundles of fibers will all contribute to simultaneous AE and EE. The slow build-up of EE prior to failure is attributed to microcracks formed on the surface, while the EE bursts in the region between 3 and 6 mm deflection are considered the result of "larger" events such as edge cracking or bundles fracturing at the front

surface. Finally, the test specimen fractures catastrophically (where the load drops), accompanied by large bursts of AE and EE occurring together. In specimens without a notch, many fibers break simultaneously with delamination - one can frequently see several plys failing successively. EE decays slowly between successive failure of the plys, but both AE and load will increase until the next catastrophic failure of more plys.

Even though some of the composite failure mechanisms described above will apply to angle ply laminates, transverse cracking and interfacial failure will predominate. When reinforcement fibers are at ± 45 degrees to the long axis, interfacial fracture is the main failure mechanism. This is clearly shown in Fig. 6 by the large simultaneous bursts of AE and EE. The EE curve is characterized by frequent bursts characteristic of crack formation which in this case is the interfacial failure at a 45 degree angle to the long axis of the sample. The EE count rate is higher when loading the sample compared to background (prior to loading). Analysis of ± 45 degree samples indicate interfacial failure on the tension side after testing. Composites with different fiber directions produce different forms of AE bursts: when composite layers are at ± 45 degrees, AE appears immediately on loading and increases with load. Interlaminar shear causes continous AE build-up. One interesting feature of AE and EE data from (0/90/90/0) degree samples is the AE build-up without any appearance of EE prior to failure. Large interlaminar shear deformation and failure will occur in 90 degree (interior) laminates prior to the failure of zero degree (exterior) laminates (Fig. 7). These events apparently cannot be detected using EE due to their being internal to the sample.

IV. CONCLUSIONS

Flexural loading of graphite-epoxy composites produces simultaneous AE and EE. A continuous AE build-up was observed from the loading of multidirectional graphite-epoxy composites. When unidirectional graphite-epoxy composites were tested, an EE build-up prior to fracture was observed. The AE build-up prior to fracture was assumed to result from accumulation of internal and external damages such as fiber breaking and interlaminar failure, as well as matrix cracking. The external failure of fibers and matrix cracking, prior to catastrophic failure, resulted in EE build-up.

The results of these experiments indicate that it is possible to detect microfractures, such as microscopic separation of tiny bundles of fibers, interfacial failure and matrix cracking in fiber-reinforced composites using EE. Even though the EE technique is not able to detect internal failure such as fiber fracture or interlaminar shear failure, it will provide evidence of failure at early stages of fracture. Also, it clarifies the source of AE as a function of strain by the presence or absence of AE-EE correlations. Comparisons of the techniques tell precisely the onset times for internal and external failure. In addition, EE technique is probably sensitive to interfacial fracture energy; higher interfacial energy will produce higher EE counts than low interfacial energy (brittle interphase). EE can thus be employed to characterize the toughness of fiber-matrix interphase in composites.

VII. ACKNOWLEDGEMENTS

First we wish to thank our Washington State University colleagues Ed Donaldson and R. V. Subramanian for their helpful discussions and contributions. We are also appreciative of interest and advice from O. Ishai, A. Gray, and L. C. Clements of the NASA-Ames Research Center.

This work was supported by the Nasa-Ames Research Center, Sandia National Laboratory, Office of Naval Research, and a grant from the M. J. Murdock Charitable Trust.

REFERENCES

1. I.G. Scott and C.M. Scalo, NDT International, April 1982, 75.

2. R. Hill, NDT International, April 1977, 63.

3. C.D. Baily, S.M. Freeman, and J.M. Hamilton, Jr., Mat. Eval., August 1980, 21.

4. A. Rotem, Fiber Sci. and Tech. 10, 102 (1977).

5. J.T. Dickinson, P.F. Braunlich, L. Larson, and A. Marceau, Appl. Surf. Sci. 1, 515 (1978).

6. D.L. Doering, T. Oda, J.T. Dickinson, and P.F. Braunlich, Appl. Surf. Sci. 3, 196 (1979).

7. L.A. Larson, J.T. Dickinson, P.F. Braunlich, and D.B. Snyder, J. Vac. Sci. Technol. 16, 590 (1979).

8. J.T. Dickinson, D.B. Snyder, And E.E. Donaldson, J. Vac. Sci. Technol. 17, 429 (1981).

9. J.T. Dickinson, D.B. Snyder, and E.E. Donaldson, Thin Solid Films 72, 225 (1980).

10. J.T. Dickinson, E.E. Donaldson, and D.B. Snyder, J. Vac. Sci. Technol. 18, 238 (1981).

11. J.T. Dickinson, E.E. Donaldson, and M.K. Park, J. Mat. Sci 16, 2897 (1981).

12. J.T. Dickinson and L.C. Jensen, J. Polymer Sci. Polymer Physics Ed. 20, 1925 (1982).

13. J.T. Dickinson, M.K. Park, E.E. Donaldson, and L.C. Jensen, J. Vac. Sci. Technol. 20, 436 (1982).

14. J.T. Dickinson, L.C. Jensen, and M.K. Park, J. Mat. Sci., 17, 3173 (1982).

15. J.T. Dickinson, L.C. Jensen, and M.K. Park, Appl. Phys. Letters 41, 443 (1982).

16. J.T. Dickinson, L.C. Jensen, and M.K. Park, Appl. Phys. Letters 41, 827 (1982).

17. H. Miles and J.T. Dickinson, Appl. Phys. Letters 41, 924 (1982).

18. L.C. Jensen, J.T. Dickinson, and A. Jahan-Latibari, "Fracto-Emission From Single Fibers of Kevlar-49," Submitted to Fibre Science Technol., 1983.

19. J.T. Dickinson, L.C. Jensen, and A. Jahan-Latibari, "Fracto-Emission: The Role of Charge Separation," Submitted to J. Vac. Sci. and Technol. 1983

20. J.T. Barnly and T. Parry, J. Phys. D: Appl. Phys. 9, 1919 (1976).

21. J. Fitz-Randolph, D.C. Phillips, P.W.R. Beaumont, and A.S. Tetelman, J. Mat. Sci. 7, 289 (1972).

22. C.K.H. Dharan, J. Mat. Eng. Tech., 100, 233 (1972).

23. R.V. Subramanian, personal communication.

FIGURE CAPTIONS

Fig. 1. Schematic diagram of experimental arrangement for EE, AE, and load measurements on composite materials in flex.

Fig. 2. EE and PIE from the tensile failure of unidirectional graphite-epoxy composites (Union Carbide Thornel 300 graphite fiber and NARMCO 5208 epoxy resin).

Fig. 3. The EE and AE accompanying the flexural straining of NARMCO 5208 bulk epoxy resin.

Fig. 4. The EE, AE, and load accompanying the flexural straining of 16 layer, unidirectional graphite-epoxy composite. (Union Carbide Thornel 300 graphite fiber and NARMCO 5209 epoxy resin.)

Fig. 5. The EE, AE, and load accompanying the flexural straining of 16 layer ($\pm$45) degree graphite-epoxy composite. (Union Carbide Thornel 300 fiber and NARMCO 5208 epoxy resin.)

Fig. 6. The EE, AE, and load accompanying the flexural straining of 16 layer, cross-ply (0,90,90,0) degree graphite-epoxy composite. (Union Carbide Thornel 300 fiber and NARMCO 934 epoxy resin.)

ORIGINAL PAGE IS
OF POOR QUALITY

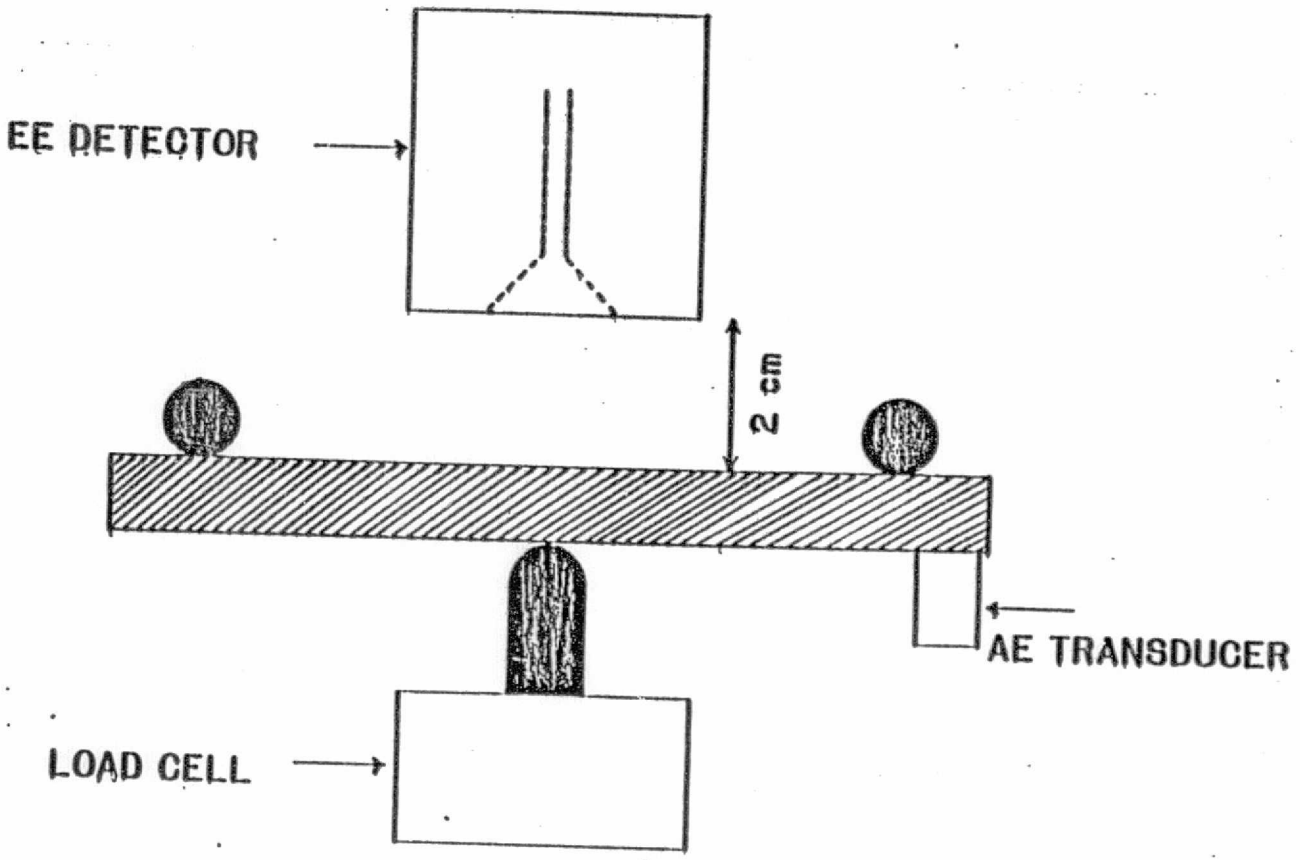

Fig. 1

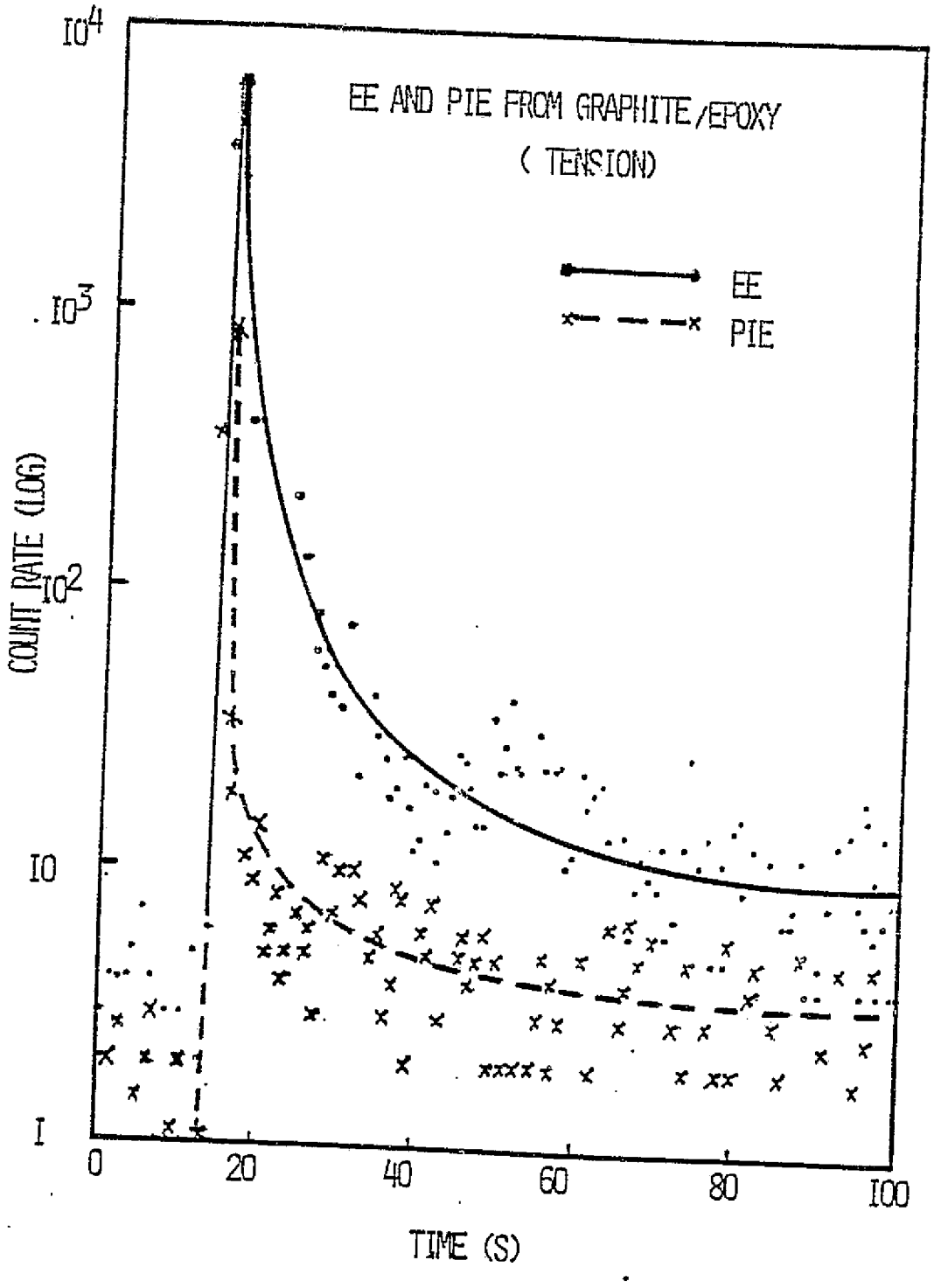

Fig. 2

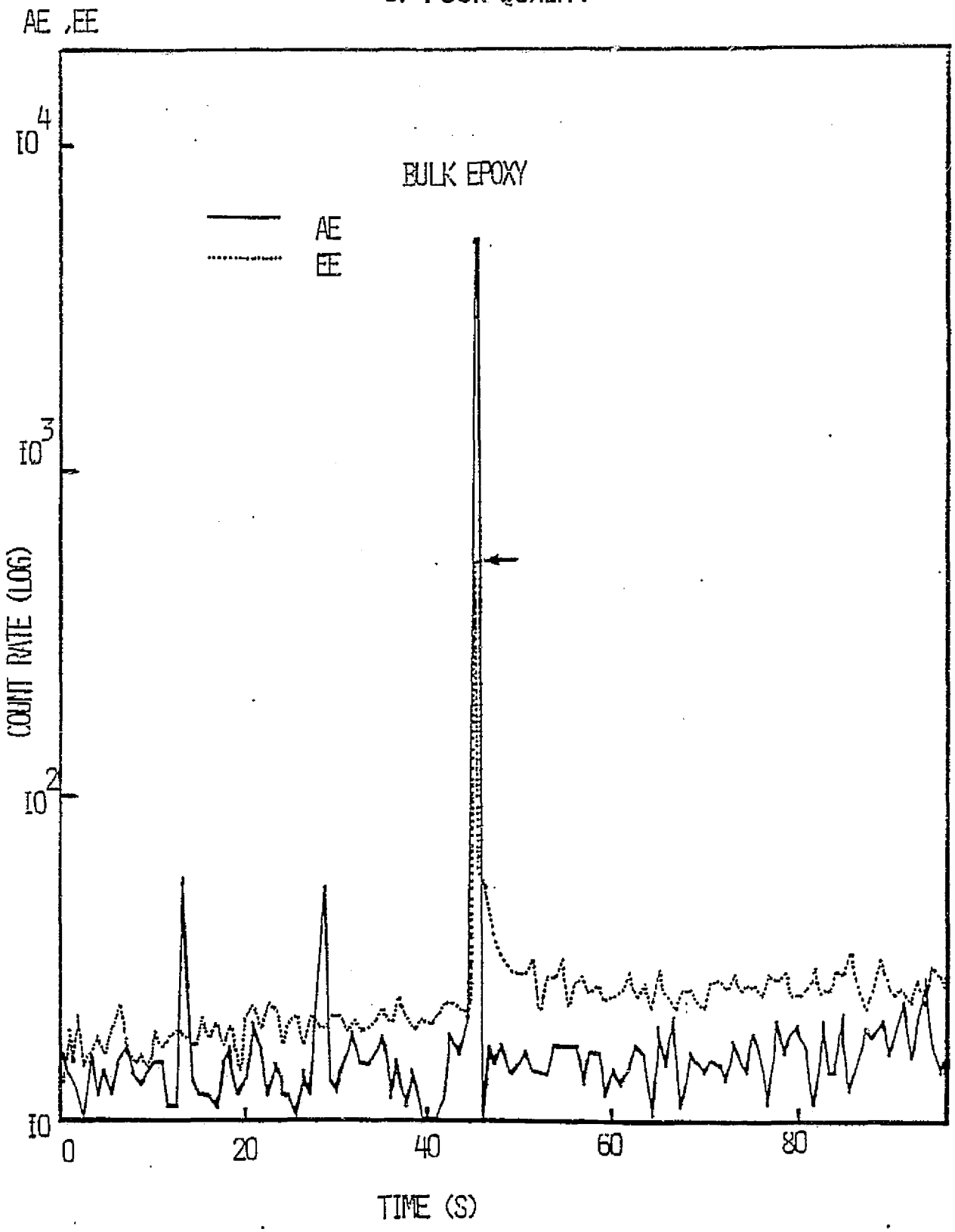

Fig. 3

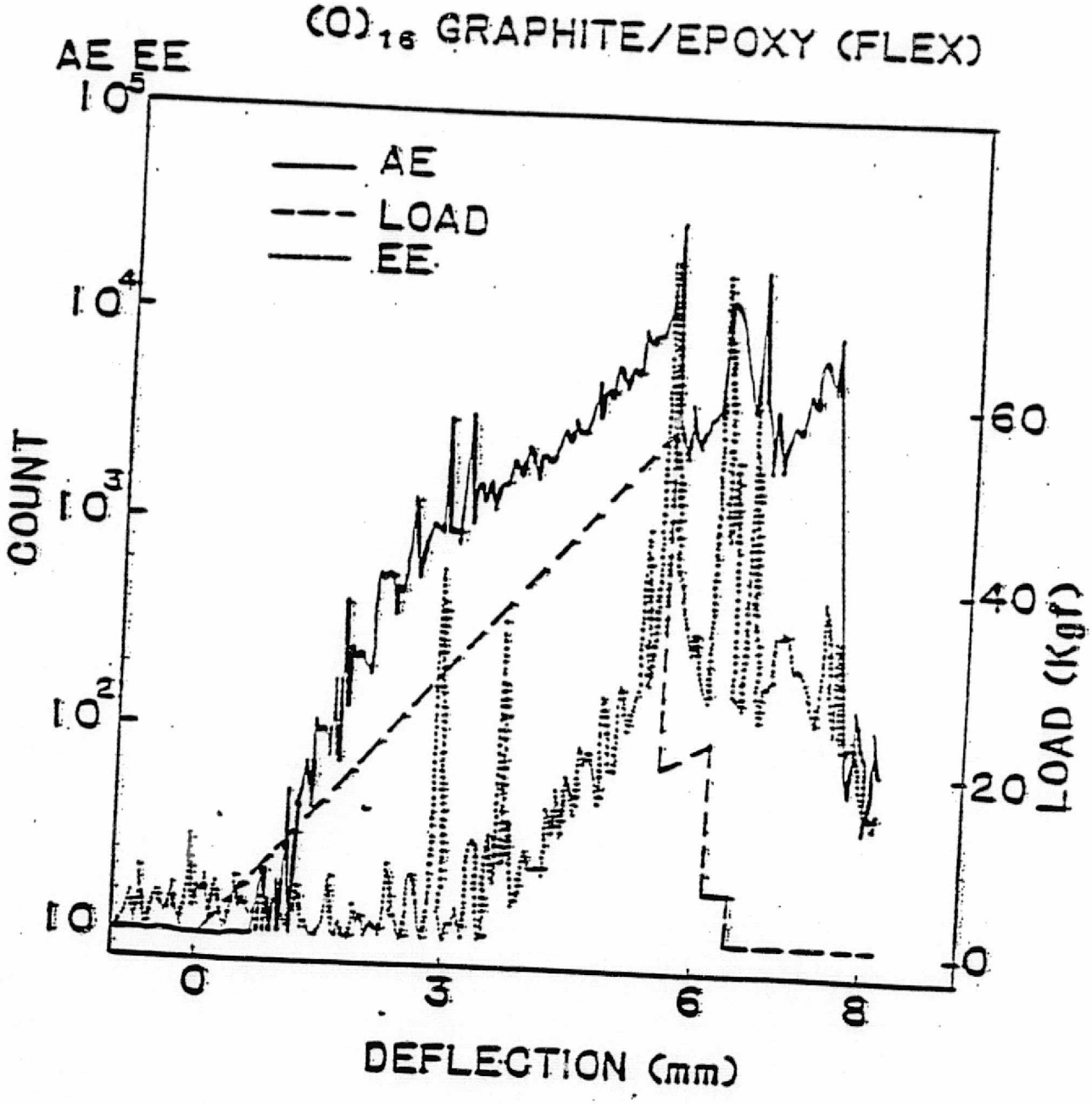

Fig. 4

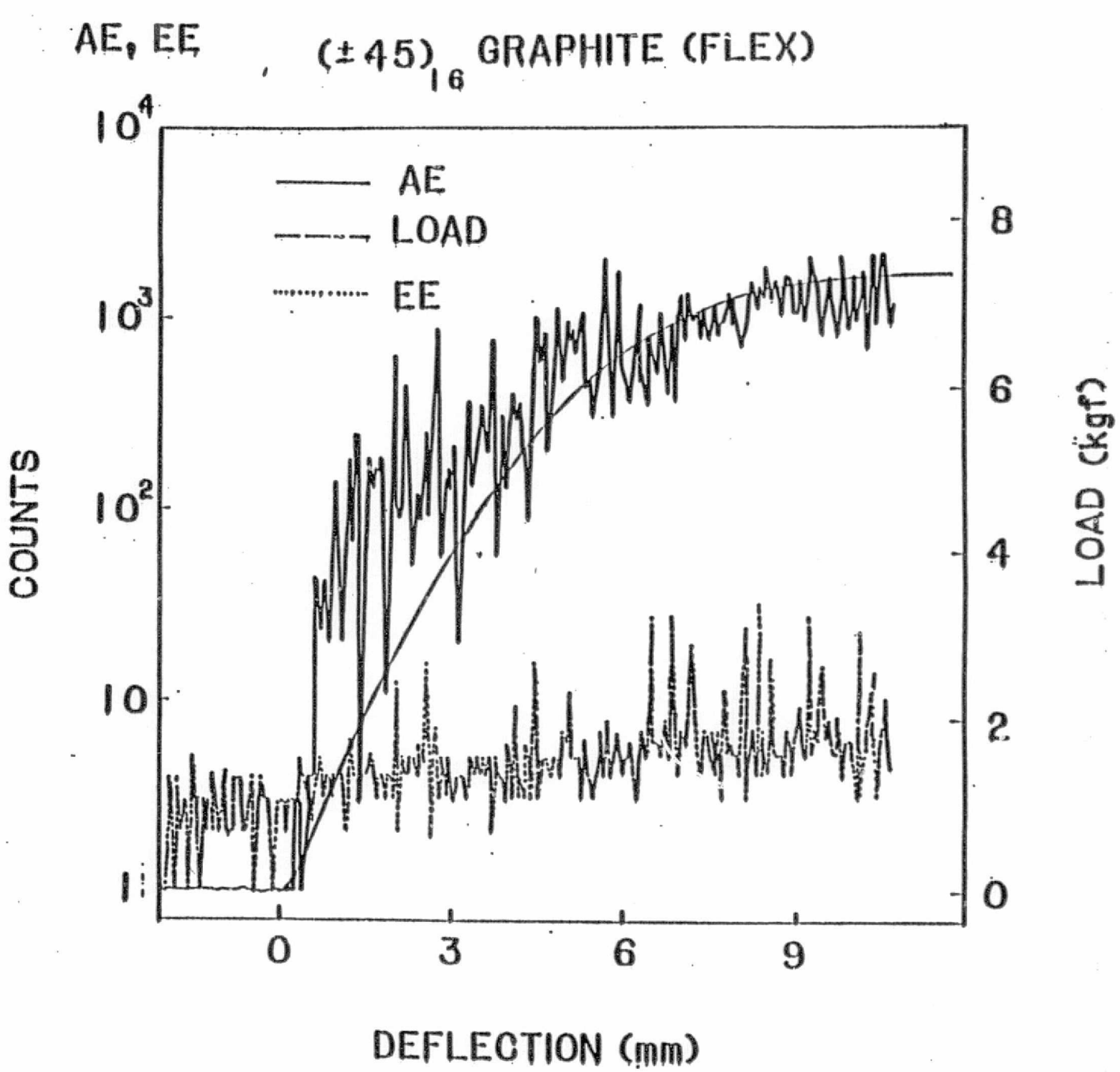

Fig. 5

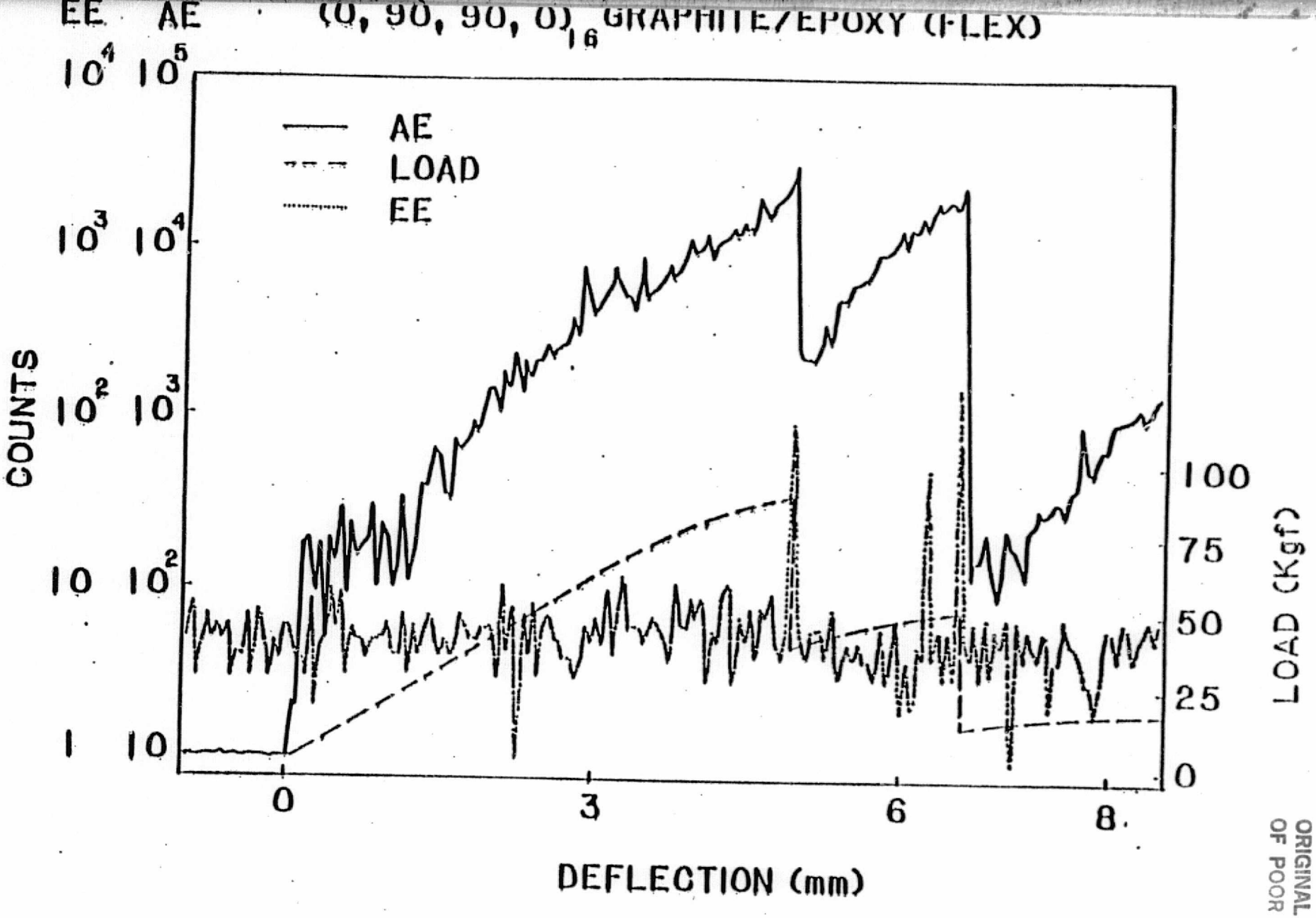

Fig. 6

IV. FRACTO-EMISSION FROM SINGLE FIBERS OF KEVLAR-49*

J. T. Dickinson, A. Jahan-Latibari, and L. C. Jensen
Department of Physics
Washington State University
Pullman, WA 99164-2814

ABSTRACT

Fracto-emission (FE) is the emission of particles (e.g. electrons, ions, and photons) during and following fracture. In this paper, we present data on electron emission (EE) and positive ion emission (PIE) from the tensile fracture of Kevlar-49 single fibers. The fibers were initially fractured in pure tension, where a stranded form of fracture was observed, often with multiple peaks spread over several hundred microseconds. The loading condition was then changed by stretching and breaking the fibers over a dull metal edge. With this change in the loading, three different forms of fracture were observed, each with its own distinctive form of emission curve. When fracture was accompanied by extensive splitting and failure between the fibrils, total emission was high and both EE and PIE decay times were long relative to fractures in which little inter-fibril failure occurred. The results of this study suggest that FE has some applicability as a tool for the detection of fracture mechanisms of single fibers.

* Trade name of E.I. Du Pont de Nemours and Co.

I. INTRODUCTION

The fracture behavior of fiber-reinforced composites is strongly dependent on the properties of the fibers, the matrix, and the interface. The role of debonding, fiber fracture, and fiber pull-out can be critical in determining the toughness of fibrous composites. Recently we have been examining various characteristics of a phenomenon called "fracto-emission," explaining its relationships to failure mechanisms in composites including fiber- and particulate-reinforced epoxies (1) as well as particulate-filled elastomers. By fracto-emission (FE) we mean the emission of particles (e.g. electrons, positive ions, neutral species, and photons) during and following the formation of a crack in a stressed material (Reference 2 and the references found therein contain our recent work on a wide variety of materials). As part of our FE studies, we have examined the FE from the fracture of single fibers of materials such as E-glass, S-glass, graphite, and Kevlar-49. The fracture properties of single fibers under tensile stress are of considerable interest because of their contribution to strength in elongation.

We report here the results of recent measurements of electron emission (EE) and positive ion emission (PIE) from the fracture of single fibers of Kevlar. In a previous study we were able to measure the mass of the PIE accompanying the fracture of Kevlar (3). In this work we focus on the time dependence and total intensities of the emission produced by such fracture. These measurements give clear indications of the time required for the fibers to undergo failure as well as the "damage" being produced during fracture. For 10 μm fibers, the time of fracture will be seen to be suprisingly long. We propose that such FE measurements may prove useful for examining the ways in

which fibers break.

II. EXPERIMENTAL PROCEDURE

The Kevlar-49 Aramid fibers used for this research are characterized by high crystallinity, high tensile strength and modulus, and low density. In the experiments to be described here, the samples were single fibers adhesively bonded to pieces of aluminum sheet shaped to fit into clamps in our vacuum system. The fiber length and diameter were 18 mm and 10 μm respectively. The fibers were strained at a rate of 1% per second until failure occurred. Almost all fibers fractured under pure tension broke in various stranded forms. For comparison, some of the fibers were stretched across a dull aluminum edge during straining; this frequently produced "smoother" fractures, with less splitting and shredding.

EE and PIE were measured using a Galileo Electro-Optics Model 4821 channel electron multiplier (CEM) positioned within 3 cm of the sample. The front of the CEM was biased at +300V for electrons and -2500V for positive ions. The pulse output (10 ns pulse width) from the CEM was amplified and fed into a 100 MHz discriminator. The resulting pulses were fed into a multichannel analyzer, allowing counts vs time to be recorded at 1 μs per channel. The emission curves varied in duration and are displayed here on various time scales, emphasizing the bursts of emission. Because of the tiny area of the fracture surface, the bursts are frequently small and the accompanying decay curves rather weak. Total particle counts are provided with each emission curve and in the tables. These may be larger than the area under the displayed curves because the after-emission is extended to longer times.

The experiments were carried out in a vacuum chamber pumped by a diffusion pump with a liquid nitrogen cold trap; the background pressure in the chamber was 1×10^{-5} Pa.

One side of the broken fiber was used to characterize the nature of the fractured fiber in terms of the degree of damage to the fiber. This was done by placing the broken fiber between two glass slides and photographing it at a magnification of 200x using a Zeiss Photomicroscope III. The "damage" was then qualitatively correlated with the intensity and time distributions of the EE and PIE from each fiber.

III. RESULTS AND DISCUSSION

Typical results of EE measurements from the purely tensile fracture of Kevlar fibers are presented in Figs. 1a and 1b. Photographs of the corresponding fracture surfaces are shown in Figs. 1a' and 1b'. As can be seen from the photographs, the fibers generally fractured into individual fibrils, a well known tendency of Kevlar fibers (4). The extent of splitting is seen to vary qualitatively between Figs. 1a' and 1b'. In Fig. 1a', the fiber fracture involves limited splitting, and the corresponding EE is of very short duration and in the form of two short bursts with a total of 308 counts. On the other hand, the fiber in Fig. 1b' is extensively split after fracture. The EE curve in Fig. 1b shows more intense, multiple bursts, characteristic of a more complicated fracture process. The emission occurred in four distinct bursts each longer in duration than the bursts in Fig. 1a. From examination of Fig. 1b' one can see that substantially more splitting and fibril fracture has occurred.

Similar results were obtained from the PIE measurements. The PIE, on the time scale shown in Fig. 2a, is characterized by multiple, long lasting bursts. Note the PIE build-up and decay of the second burst in Fig. 2a (about 100 μs). This relatively slow build-up of the emission is most likely an indication of the time required for the splitting or separation process for the formation of the individual fibrils, while the decay time or after emission is due to thermally stimulated relaxation of the fracture surfaces (6). This is supported by the splitted form of fracture shown in Fig. 2a'. It is obvious from Figs. 1 and 2 that both EE and PIE are more intense when fibers fracture into separate fibrils.

These emission curves and photographs (Figs. 1 and 2) show the complicated forms of fracture that occur from the tensile deformation of Kevlar single fibers. In Table I we have summarized the total emission counts for a 1 millisecond interval during and after fracture, the number of distinguishable EE or PIE bursts (peaks), and the time duration between the occurence of the first burst and the last burst. This time is an indication of the time from initial fiber damage to final failure for the slow strain rate used in this experiment. What is surprizing is the magnitude of this time in relation to the small cross-sectional area of the sample. In general, from the parameters in Table I, we see that when the total emission for either EE or PIE is high the splitting and formation of fibrils is significant, and there is evidence of extensive plastic deformation (as observed with the photomicroscope). Also, a high total emission count was generally accompanied by bursts of EE or PIE with long decay. We tentatively suggest that long after-emission may be related to a higher degree of fibril formation and/or plastic deformation.

This form of fracture, namely the splitting and formation of fibrils, was

previously seen by Chiao, et al. (4) while testing Kevlar/epoxy strands. Chiao, et al. also detected particles or defects within the fibrils which did not appear to be artifacts, but were an inherent characteristic of the fiber. Due to the presence of these defects, some fibrils fracture at a lower stress level than others, producing an initial fracture in different parts of the fiber, followed by failure of the stronger fibrils at later times. This form of fracture might thus yield successive bursts of emission over measurable time periods. At this point, we can not distinguish clearly the order of events producing the sequence of EE bursts that we observe.

Fig. 3 shows typical EE measurements and corresponding photographs of Kevlar-49 single fibers stretched and broken over the dull metal edge. Similar results of PIE measurements and photographs of their respective fracture surfaces are presented in Fig. 4. Although each graph or photograph in Figs. 3 or 4 is for a particular fiber, they are representative of approximately fifty samples we studied.

For samples broken across the metal edge, three distinctive forms of fracture can be qualitatively distinguished by the examination of the emission curves and the photographs. The first type was characterized by low total emission followed by a rapid decay; this corresponded to a "clean" fracture where the fiber cleaved relatively cleanly across its cross-section (see Figs. 3a and 3a', 4a and 4a'). Second, a "splitting" type of fracture was observed which was accompanied by greater counts of both EE and PIE, with longer decay times (see Figs. 3b and 3b', 4b and 4b', and Table II). This form of fracture was the type that dominated when fibers were fractured in pure tension. In the third form of fracture, the fiber broke mainly across its cross-section, but the resulting fracture surfaces are frayed. Such "frayed" fracture was

characterized by several bursts of electrons and positive ions, with some bursts lasting up to 200 μs (see Figs. 3c and 3c', 4c and 4c').

Table II presents average values of the parameters; total counts, number of bursts, and time duration to characterize typical behavior for each type of fracture.

In Kevlar fibers the extended polymer chains along the fibril axes are covalently bonded, whereas the fibrils are attached to one another in the transverse direction only by hydrogen bonds (5). The weak hydrogen bonds break easily and cause the fibrils to separate from one another during fracture. When the fiber fracture is "clean", a limited number of either covalent or hydrogen bonds were broken. In addition, the exposed fiber surface area is very small. Therefore the total emission count is low with a very rapid decay (see Figs. 3a and 4a). In cases where fibrils are formed extensively even though the total number of failed covalent bonds may be no higher than that found in flat fracture, a very high number of hydrogen bonds are broken. The failure of hydrogen bonds causes more fibril surface area to be exposed and may produce charge separation in a way similar to delamination or "interfacial failure," which we have found produces intense emission (2,6). We have shown that charge separation during fracture plays a key role in the emission mechanism; in general, when charge separation is intense so is the EE and PIE (2,6). Thus the FE may be providing signals indicative of the manner in which the fibers are failing.

IV. CONCLUSIONS

The emission of electrons and positive ions from the fracture of single

fibers of Kevlar-49 has been examined on the microsecond time scale. Evidence of the time required from initial damage to ultimate failure of the fiber has been provided, showing times ranging from a few microseconds to several hundred microseconds. Secondly, the total emission from the entire fracture event tends to correlate with the extent of "damage" to the fiber produced by fracture. Finally, by examination of the shape and intensity of the EE/PIE bursts, it may be possible to differentiate between fibril formation vs fibril fracture. A measurement of other EE/PIE characteristics such as kinetic energy or use of other FE components (e.g. neutral emission or photon emission) might provide more deformation information on the fracture processes occurring where such fibers are stressed to failure.

V. ACKNOWLEDGMENTS

We would like to express our gratitute to our Washington State University colleagues, W. E. Johns and W. Plagemann, for assistance and the use of the Zeiss Photomicroscope III, and B. H. Carroll for assistance in preparing this manuscript. We also wish to thank R. L. Moore, Lawrence Livermore Laboratory, for the samples of Kevlar fiber.

This work was supported by the NASA-Ames Research Center, the National Science Foundation, McDonnell-Douglas Corporation, and a grant from the M. J. Murdock Charitable Trust.

REFERENCES

1. J.T. Dickinson, A. Jahan-Latibari, and L.C. Jensen, to appear in Proceedings of the "Symposium on Composites, Interfaces", ACS Seattle, 1983.

2. M.H. Miles and J.T. Dickinson, Appl. Phys. Lett. 41, 924 (1983).

3. J.T. Dickinson, L.C. Jensen, and M.K. Park, J. Mat. Sci. 17, 3173 (1982).

4. T.T. Chiao, M.A. Hamstad, M.A. Marcon and J.E. Hanafee, "Filament-Wound Kevlar-49/Epoxy Pressure Vessels," NASA CR-134506 final report, Lawrence Livermore laboratory.

5. L. Penn and F. Larson, J. Appl. Poly. Sci. 23, 59 (1979).

6. J.T. Dickinson, L.C. Jensen, and A. Jahan-Latibari, "Fracto-Emission: The Role of Charge Separation," Submitted to J. Vac. Sci. Technol., 1983.

Table I. Selected Parameters for Electron and Positive Ion Emission From the Fracture of Kevlar Single Fibers.

Emission Type	Total Emission Counts Per 1 ms	Number of bursts	Time Duration* (Microseconds)
EE	308	5	681
	615	4	125
	640	3	209
	860	4	116
	576	3	132
	264	2	147
	429	3	111
PIE	1265	3	219
	195	1	-
	882	2	19
	744	4	59

* Time between the occurrence of the first and last burst

Table II. Averages of Selected Parameters of EE and PIE for Various Forms of Kevlar-49 Single-Fiber Fracture. (Fibers Stressed Over Metal Edge.)

Fracture Microstructure	Emission Type	Total Emission Counts per 1 ms)	Number of Bursts	Time Duration* (Microseconds)
Clean	EE	334	3	15
	PIE	42	1	-
Stranded	EE	470	2	25
	PIE	641	2	6
Frayed	EE	1168	6	5390
	PIE	768	4	470

* Time between the occurrence of the first and last burst

FIGURE CAPTIONS

Fig. 1: Electron emission and photographs of fracture surfaces of Kevlar single fibers fractured in pure tension: a) limited splitting, and b) extensive splitting of fibrils.

Fig. 2: Positive ion emission and photographs of the corresponding fracture surfaces of a Kevlar single fiber fractured in pure tension.

Fig. 3: Electron emission and photographs of the corresponding fracture surfaces of Kevlar single fibers fractured across a dull metal edge: a) flat, b) stranded, and c) frayed fracture.

Fig.4: Positive ion emission and photographs of the corresponding fracture surfaces of Kevlar single fibers fractured across a dull metal edge: a) flat, b) stranded, and c) frayed fracture.

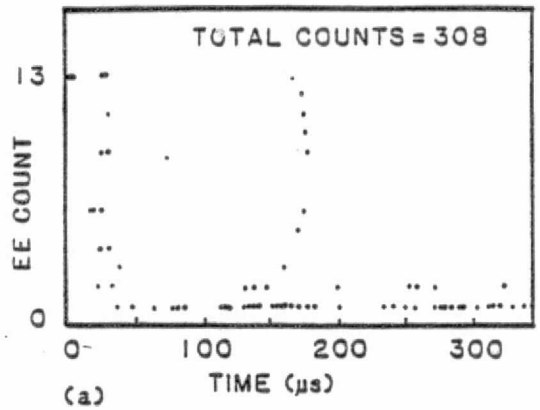

(a)

(a')

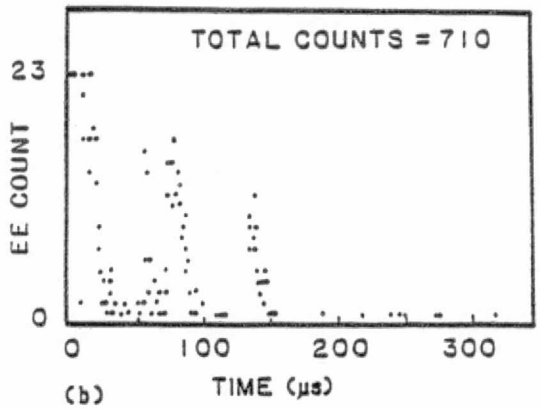

(b)

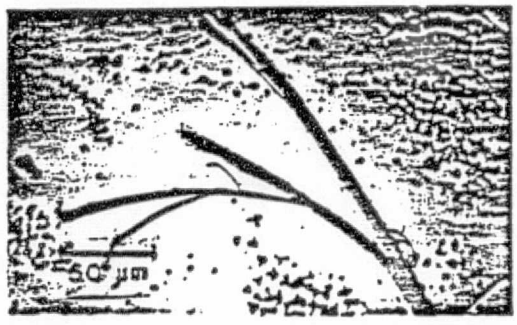

(b')

(a)

(a')

Fig. 2

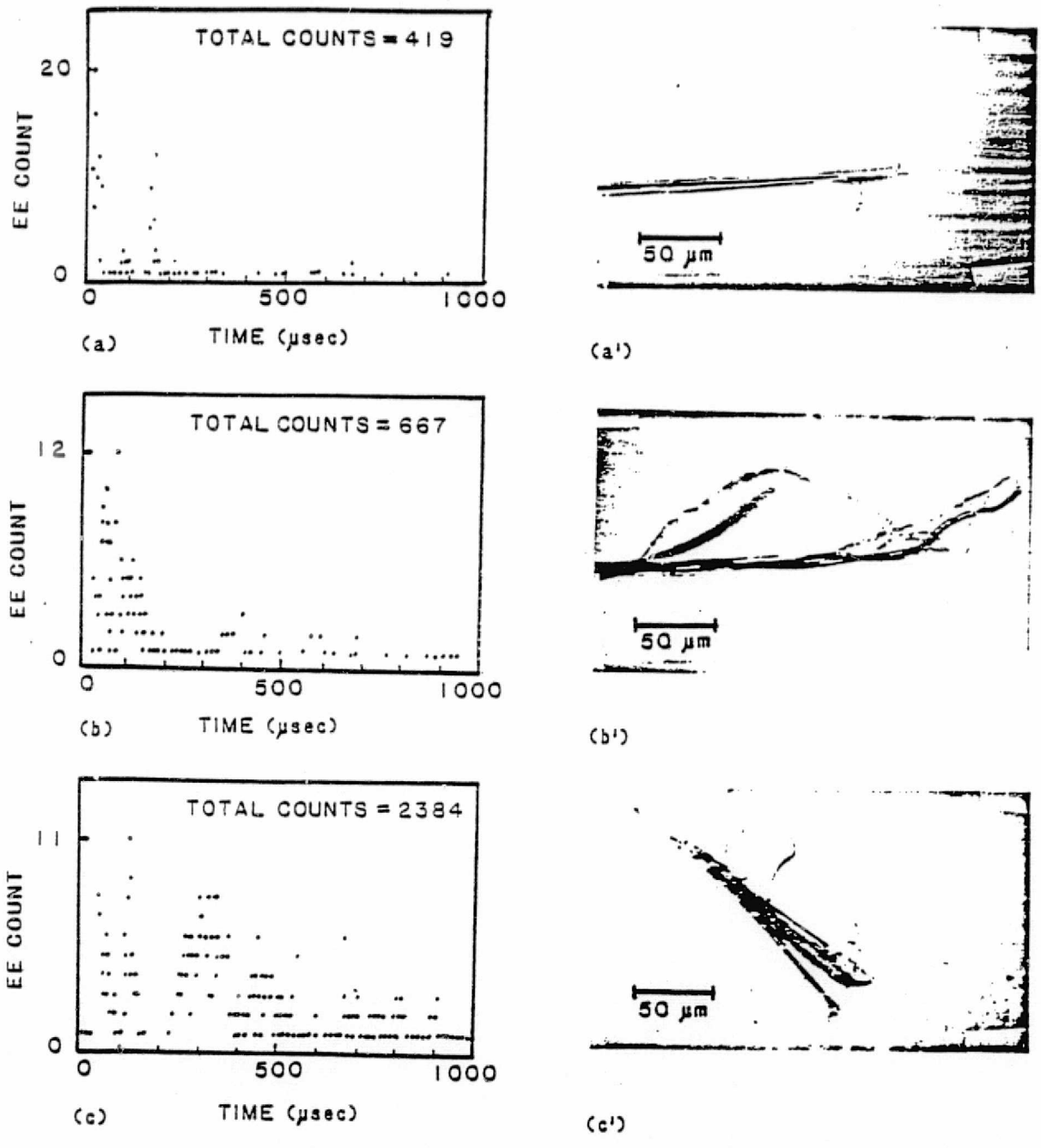

Fig 7

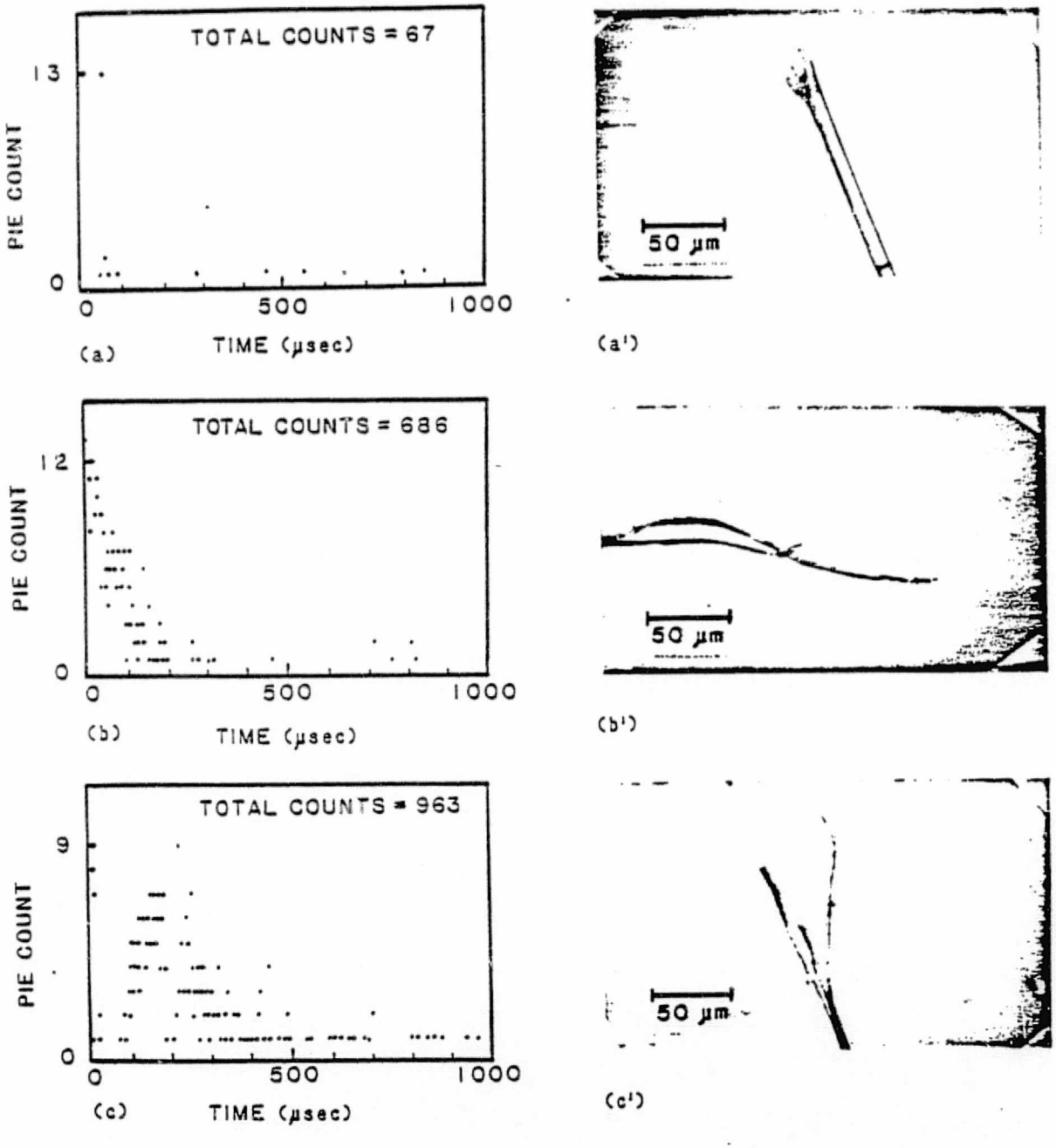

Fig. 4

V. FRACTO-EMISSION: THE ROLE OF CHARGE SEPARATION

J. T. Dickinson, L. C. Jensen, and A. Jahan-Latibari
Department of Physics
Washington State University
Pullman, WA. 99164-2814

ABSTRACT

Fracto-emission is the emission of particles (e.g. electrons, ions, ground state and excited neutrals, and photons) during and following fracture. We have found that during fracture of adhesive bonds and crystalline materials involving large amounts of charge separation on the surface, the emission of charged particles, excited neutrals, light, and radio waves occurs with unique and revealing time dependencies. In this paper we report simultaneous fracto-emission measurements on several systems. We interpret the results in terms of a conceptual model involving the following steps: (1) charge separation due to fracture, (2) desorption of gases from the material into the crack tip, (3) a gas discharge in the crack, (4) energetic bombardment of the freshly-created crack walls, and (5) thermally stimulated electron emission, accompanied by electron stimulated desorption of ions and excited neutrals. In addition to evidence from fracture experiments, we present results from studies of electron bombardment of a polymer surface.

I. INTRODUCTION

Fracto-emission (FE) is the emission of particles (e.g. electrons, ions, ground state and excited neutrals, and photons) during and following fracture of materials. In past work we have observed intense, long-lasting emission of electrons (EE) and positive ions (PIE) from systems where high densities of surface charge develop on the fracture surface (see references contained in reference 1). Such systems include: 1) adhesive failure (e.g. peeling of pressure-sensitive adhesives from inorganic substrates, fracture of particulate-filled elastomers, fracture of fiber-reinforced epoxies), 2) fracture of piezoelectric materials such as crystalline SiO_2, sucrose, and polycrystalline PZT, and 3) a number of non-piezoelectric materials which still show intense charge separation, such as LiF, MgO, Al_2O_3, and mica.

In examining the various components of FE from these materials we found it useful to measure simultaneously two or more types of emission on various time scales, to provide further understanding of the emission mechanisms. Some of this work has been previously described for EE and PIE from polybutadiene filled with glass beads. The results previously obtained can be summarized as follows:

1. EE and PIE rise rapidly together during crack propagation, and decay immediately after separation of the fracture surfaces with identical kinetics (2-4).

2. On a submicrosecond time scale, a substantial fraction of the PIE

is in coincidence with the EE (3-5). This suggests that at least some of the electrons emitted are either created simultaneously with positive ions, or more likely, creation of the positive ions is accompanied by inelastically scattered electrons and/or Auger electrons from an ESD-like process (7).

3. There are neutral species emitted from materials undergoing fracture (6). These can be attributed to the release of absorbed species and/or fracture fragments (decomposition).

4. There are also excited neutrals emitted which are correlated in time with the EE (4). We have attributed these metastable molecules to ions neutralized in the process of leaving the surface.

In this paper we would like to report recent results involving simultaneous measurement of EE, photons (phE), and radio waves (RE) accompanying the fracture in vacuum of various materials where strong charge separation occurs. Also, measurements of EE and PIE induced by electron bombardment are presented for one material, polybutadiene. Finally a conceptual model is presented that ties together these new observations and those summarized above.

II. EXPERIMENTAL

The measurements described here were performed on materials fractured in a vacuum of 1×10^{-5} Pa. Samples were fractured either in tension or in three point flexure. The alumina-filled epoxy consisted of one part by weight EPON 828 (Z-hardener) epoxy to three parts of irregularly-shaped alumina particles with an average diameter of 10 μm. The 2mm X 17mm X 45mm samples

were notched with a sharp saw and fractured in tension in front of the detectors. The polybutadiene (BR) consisted of Diene 35NFA (Firestone Tire and Rubber Co.) crosslinked with 0.05% (by weight) dicumyl peroxide by heating for 2 hours at 150 °C. Some BR samples contained 30-95 μm glass beads (34% by volume). Samples were 2mm X 5mm X 20mm, and were notched slightly in the middle as before. The sucrose crystals were grown by allowing a saturated solution of sugar in water to evaporate for three weeks. These crystals were broken by applying a force perpendicular to the piezoelectric axis. Sucrose and quartz crystals were fractured in flexure. BR for electron bombardment studies consisted of Diene 35NFA dissolved in benzene and allowed to evaporate on a supporting Cu sheet. This resulted in a 0.8 mm thick BR film covering the Cu sheets. The SiO_2 crystals were x-cut disks, 6.5 mm in diameter by 1.2 mm thick, the disk face being the $(\bar{2},1,1,0)$ plane. The fracture surfaces tended to be perpendicular to the disk face.

The electrons were detected with a channeltron electron multiplier (background noise counts ranged from 1 to 10 counts per second). A Bendix BX754A Photon Counter Tube with an S-20 photosensitive surface and background count rate of 10-20 counts per second was used to detect visible photons. The two detectors were generally placed within 1 cm or less from the region where the crack would propagate. Both detectors yielded 10 ns pulses which could be treated with standard pulse counting techniques and stored in a multi-channel analyzer (MCA).

In addition to EE and phE, we detected the emission of radio frequency electromagnetic waves (RE) accompanying fracture in vacuum. RE has been detected previously by Derjaguin, et al. (8) during the separation of polymer films from dielectric surfaces at pressures considerably higher (10^3 -

10^5 Pa) than ours (10^{-5} Pa). The RE was detected using two different pickup coils: a 2.5 mH RF choke coil and a 20000 turn solenoid of No. 30 magnet wire. Either coil was connected to the input of a wide-band differential amplifier with high common mode rejection to minimize pick-up noise, and further amplified by a second amplifier. The response of each coil to a fracture event was a ringing signal with approximate frequencies and duration as follows:

2.5mH choke coil	600 khz	20 μs
20000 turn solenoid	8 khz	1 ms

The solenoid was 5 times more sensitive but because of the higher inductance and thus longer ringing it could only be used to determine the onset of detectable RE or the actual occurrence of RE emission, with approximate values of RE duration. The choke coil allowed more accurate time correlations but with reduced sensitivity.

Two methods of recording RE were used: the choke coil signals were fed into a discriminator, so that rings above a threshold produced pulses which were then counted with an MCA, thereby detecting the presence of bursts of RE as a function of time. The second method, used for the solenoid, consisted of digitizing the coil output with a wave-form digitizer. The rise of the RE ringing signal could then be correlated in time with other FE by the use of synchronized start pulses. Thus within one channel width on the MCA all three FE components could be compared. Previous experiments (2) correlating FE to video recording of crack growth indicated that EE intensity rises rapidly during crack propagation and falls upon separation of the fracture surfaces.

Although it has not been proven conclusively for rapid crack growth, we have assumed that the most intense EE is occurring during crack propagation.

III. RESULTS

The first set of data, shown in Fig. 1, is from the fracture of alumina-filled epoxy. The time scale chosen was in an intermediate range to assure aquisition of all three signals and still provide reasonably good time correlation information. In a separate experiment measuring crack motion in this material with a rotating framing camera, the duration of crack growth was found to be about 20 μs. The data in Fig. 1 was taken at 40 ms per channel and the count rate is plotted on a log scale vs. time. The EE burst occurring during fracture, seen in Fig. 1 as the point where the EE count rate is a maximum, is accompanied by a burst of RE as well as phE. The phE may show a weakly-defined tail; the RE drops off immediately after fracture. The results shown here were reproducible for 10 consecutive samples and show that in a vacuum there is an electrical breakdown occuring during fracture of this filled polymer.

Figs. 2-4 show similar results for polybutadiene (BR) filled with glass beads, single-crystal sucrose, and single-crystal quartz. All show the burst of RE and phE accompanying fracture. The BR and SiO_2 show clear evidence of tails following fracture, which may to a first approximation follow the electron decay in form. Note that for the filled BR we were able to follow phE and EE rising together, due to the much slower crack velocity. Also note that the drop in phE after the peak is for all of these material far more than a simple proportionality relative to the drop in EE; i.e., the phE during

fracture is much more intense than a phE mechanism that remains parallel to an EE mechanism would predict.

As a further test of the occurrence of a discharge during fracture, simultaneous PIE and RE measurements were taken for the fracture of the filled BR using the more sensitive solenoid coil (PIE was measured rather than EE because on faster time scales EE showed evidence of saturating the electron multiplier.). Of primary interest here was the onset of RE relative to the growth of PIE which we know rises with EE during fracture. The time of fracture has been reduced (by increasing the strain rate by approximately a factor of twenty) in order to increase the amplitude of the RE during fracture. The digitized waveform of the RE signal was squared, averaged, and the background subtracted to yield the average power in the ringing RE signal. This result is shown with the corresponding PIE count rate for the filled BR in Fig. 5, where great care has been taken to align the curves correctly in time. The RE is seen to break out of the background noise in the regions of most intense electron emission. The arrows indicate bursts of PIE and RE that are correlated in time. Also, the regions where the PIE is most intense correspond to regions where the RE is highest, where it has been shown (8) that the crack velocity is the highest. Thus, it appears that the RE intensity is velocity dependent also. The primary result here is that we can see RE during a considerable portion of the period in which we observe PIE.

In anticipation of a component of EE possibly produced by bombardment of the fracture surface by charged particles created in a discharge, we performed two experiments on a thick film of BR. At room temperature, the BR was bombarded with with 2 keV electrons at nanoampere currents for 5 minutes. As soon as the electron beam was turned off, a nearby channeltron biased to detect

electrons was turned on. Fig. 6a shows the resulting EE, with a long-lasting decay which is very similar to that of EE induced by fracture. This effect has been extensively studied on crystalline inorganic materials, such as oxides and alkali halides and is known as thermally stimulated electron emission (TSEE)(9). Here we see (to our knowledge for the first time) the same phenomenon, TSEE, at room temperature from a polymer.

Because of our extensive studies of fracture-induced PIE from this material (3,4), we also examined the emission of ions both during and after electron bombardment. For an energy of 2 keV and a current of 5 nanoamperes we see in Fig. 6b the PIE emitted during bombardment, which decays away as soon as the bombardment stops. The ions are not following a parallel mechanism to the EE but are following an ESD mechanism only. Thus we propose that the PIE observed during fracture is due to a portion of the EE which never completely escapes the sample but rather collides with the surface (probably at positive charge patches) and induces ESD of positive ions.

IV. CONCEPTUAL MODEL

At least in the cases illustrated here where significant charge separation occurs during fracture, we feel that the gaseous discharge that we detected using RE and phE is playing a very important role in the production of EE and PIE. In fact, variations in discharge intensity may explain the large variation in intensities observed for a wide range of materials, crack velocities, and other factors. The basic ideas we are proposing are:

1. The fracture event yields charge separation (usually patchy) producing an electric field, E, in the crack.

2. Desorption of volatiles and/or fracture products raises the pressure, P, in the crack tip.

3. A gas discharge (dictated by P, E, and a distance d which characterizes the crack width) occurs, producing the RE and phE. Electron and ion bombardment of the crack walls occurs during this discharge.

4. Bombardment of the fracture surfaces creates primary excitations, usually explained in inorganic crystals in terms of electron-hole production raising electrons into traps near the conduction band, which then undergo thermally stimulated migration until recombination with a hole occurs. This recombination can yield an emitted electron (thermally stimulated electron emission (TSEE)), say by an Auger process, or a photon (thermal luminescence, (TL) (12)).

5. A portion of the electron emission strikes adjacent patches of positive charge yielding PIE via an ESD mechanism. Some of these positive ions are neutralized as they leave the surface yielding the excited neutral component of FE that we have observed.

Consistent with this model are the observations that qualitatively, when charge separation is intense, so are EE and PIE. Secondly, the RE and phE peak intensities (i.e., during fracture) appear to be closely following the same trends. Third, in materials where charge separation is intense but the RE is weak, the EE and PIE tend to be small (e.g. an alkali halide). Fourth, the very close tie between EE and PIE count rates following fracture supports the ESD mechanism. Furthermore, the PIE kinetic energies we observe are often in the hundreds of eV (10,11) suggesting that the PIE originates from positive charge patches. Fifth, coincidence experiments showed that there was a finite probability of detecting an electron in close coincidence with an emitted

positive ion. This electron could be an inelastically scattered electron (creating the ESD excitation) or an accompanying Auger electron expected in the ESD process involving creation of a core hole. Sixth, in the case of sucrose and SiO_2 there is an observable phE decay that follows the EE decay after separation of the fracture surfaces, indicating a parallel de-excitation mechanism, similar to what is observed in TSEE and TL. Finally, the strong increase in EE with crack velocity observed in filled BR would be expected because: a) the surface charge densities may be higher due to the reduced reneutralization through conduction paths, and b) increased gas desorption into the crack tip occurs due to an expected increase in crack tip temperature with crack velocity.

V. CONCLUSIONS

These initial results and this conceptual model allow us to make a number of predictions concerning the dependence of fracture-induced EE on material properties, temperature, and crack velocity. Also, quantitative models relating various FE intensities to measurement of surface charge (measured in vacuum), surface conductivity, and separate TSEE, TSL, and ESD should be possible. We are currently pursuing these and a number of other features of fracture-induced particle emission.

VI. ACKNOWLEDGMENTS

The authors would like to express their gratitude to Alan Gent, University of Akron Institute of Polymer Science for contributing the BR samples and Lydia Brix, a Washington State University physics undergraduate, for growing the sucrose crystals. We also wish to thank B. H. Carroll for assistance in preparing this manuscript. This work was supported by the National Science Foundation, the Office of Naval Research, Sandia National Laboratory, NASA-Ames Research Center, and the M.J. Murdock Charitable Trust.

REFERENCES

1. H. Miles and J. T. Dickinson, Appl. Phys. Lett. 41, 924 (1982).

2. J. T. Dickinson and L. C. Jensen, J. Polymer Sci. Polymer Physics Ed. 20, 1925 (1982).

3. J. T. Dickinson, L. C. Jensen, and M. K. Park, J. Mat. Sci. 17, 3173 (1982).

4. J. T. Dickinson, L. C. Jensen, and M. K. Park, Appl. Phys. Lett. 41, 443 (1982).

5. J. T. Dickinson, L. C. Jensen, and M. K. Park, Appl. Phys. Lett. 41, 827 (1982).

6. L. A. Larson, J. T. Dickinson, P. F. Braunlich, and D. B. Snyder, J. Vac. Sci. Technol. 16, 590 (1979).

7. M. L. Knotek and P. J. Feibelman, Phys. Rev. Lett. 40, 964 (1978).

8. B. V. Derjaguin, L. A. Tyurikova, N. A. Krotova, and Y. P. Toporov, IEEE Transactions on Industry Applications IA-14, 541 (1978).

9. J. A. Ramsey, "Exoelectron Emission," in Progress in Surface and Membrane Science 11 (Academic Press, New York 1976) pp. 117-180.

10. J. T. Dickinson, E. E. Donaldson, and M. K. Park, J. Mat. Sci. 16, 2897 (1981).

11. J. T. Dickinson, M. K. Park, E. E. Donaldson, and L. C. Jensen, J. Vac. Sci. Technol. 20, 436 (1982).

12. R. Chen and Y. Kirsh, Analysis of Thermally Stimulated Processes, (Pergamon Press, New York, 1981), pp. 48-52.

FIGURE CAPTIONS

Fig. 1: Simultaneous emission of electrons, photons, and radio waves from the fracture of alumina-filled epoxy.

Fig. 2: Simultaneous emission of electrons, photons, and radio waves from the fracture of polybutadiene filled with small glass beads.

Fig. 3: EE, phE, and RE from the fracture of single-crystal sucrose.

Fig. 4: EE, phE, and RE from the fracture of SiO_2.

Fig. 5: PIE and RE during fracture of filled BR. Note the fast time scale.

Fig. 6: Consequences of electron bombardment on BR: a) EE following bombardment, and b) PIE during bombardment.

FE FROM Al_2O_3 FILLED EPOXY

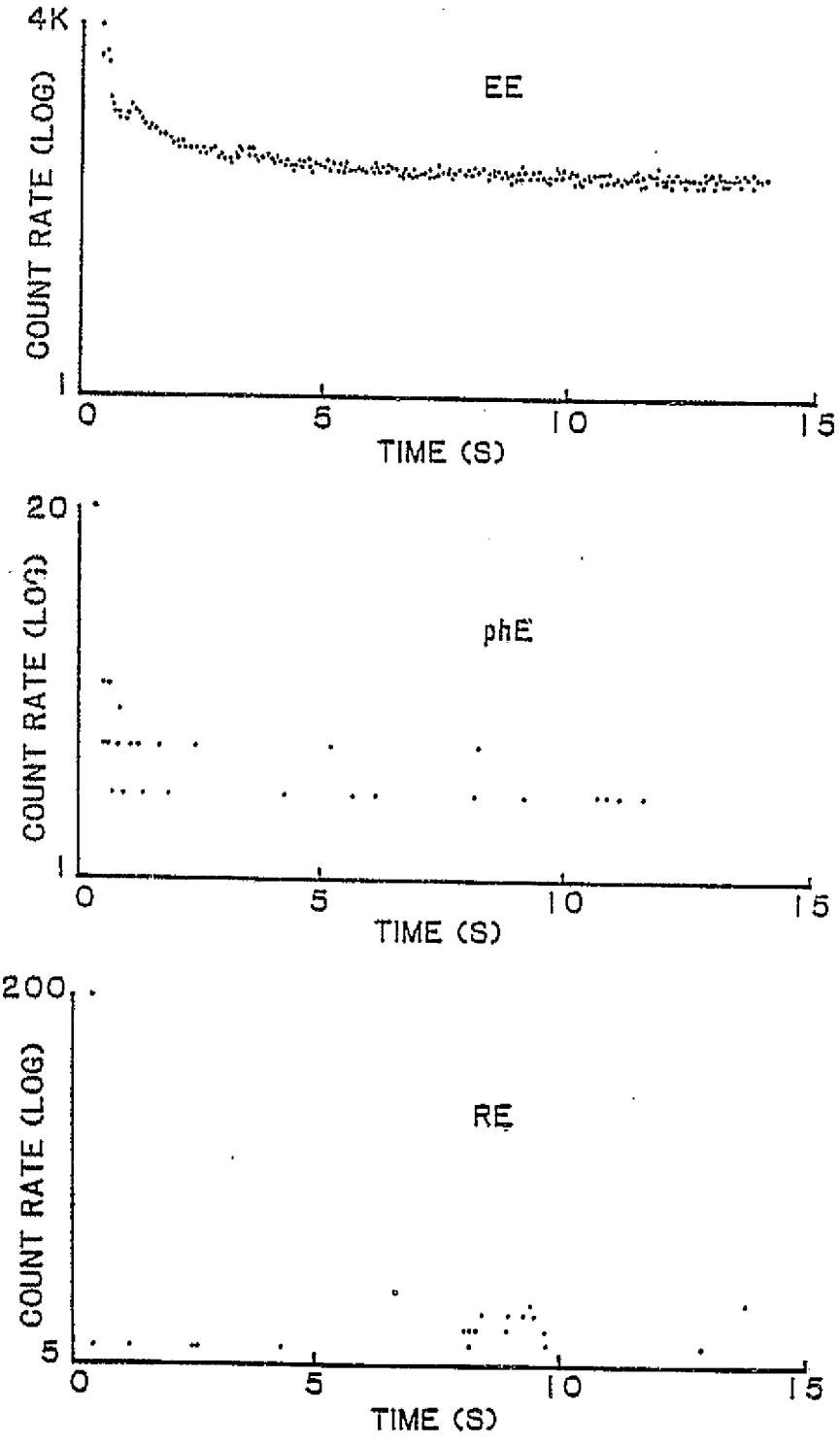

Fig. 1

FE FROM BR FILLED WITH GLASS BEADS

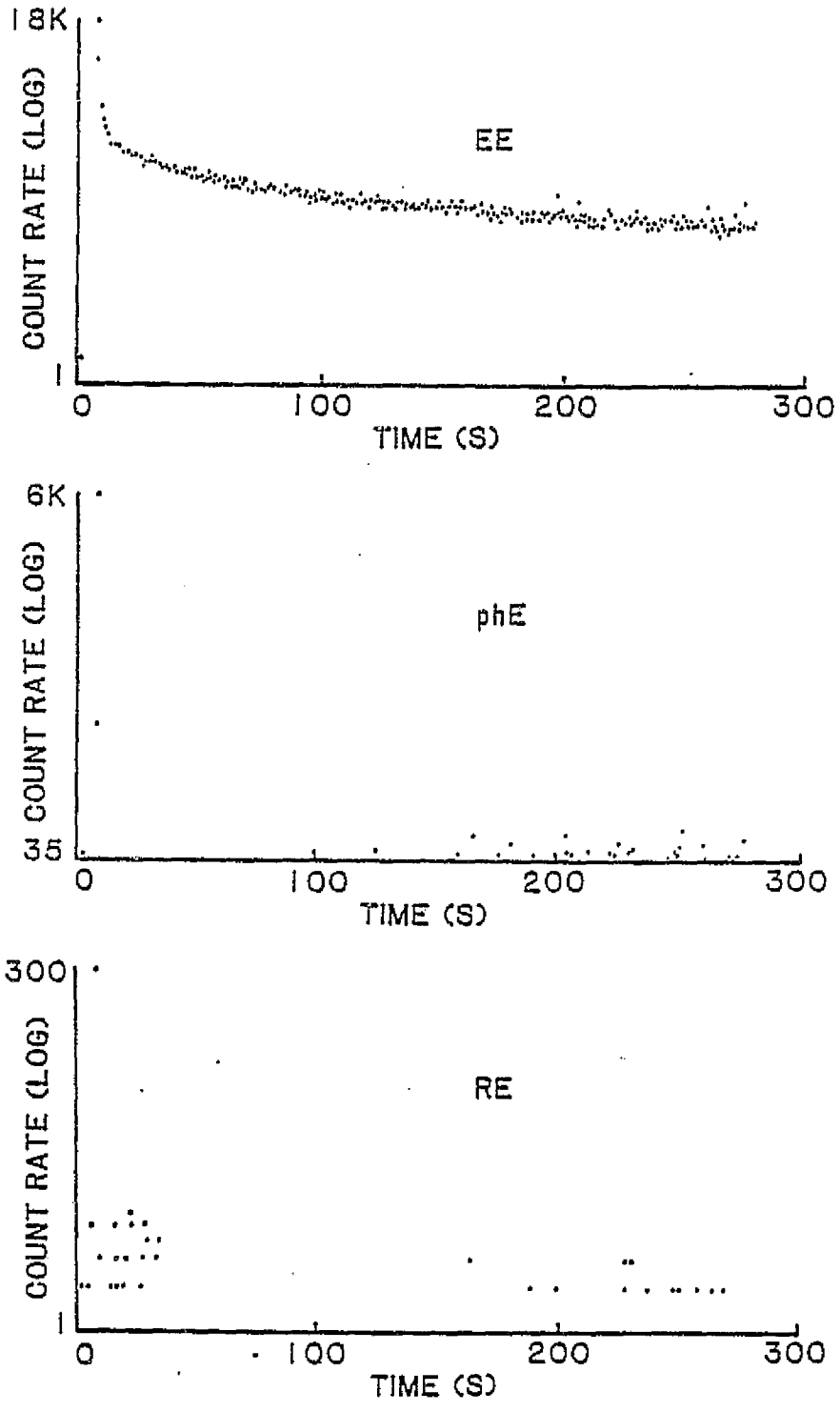

Fig. 2

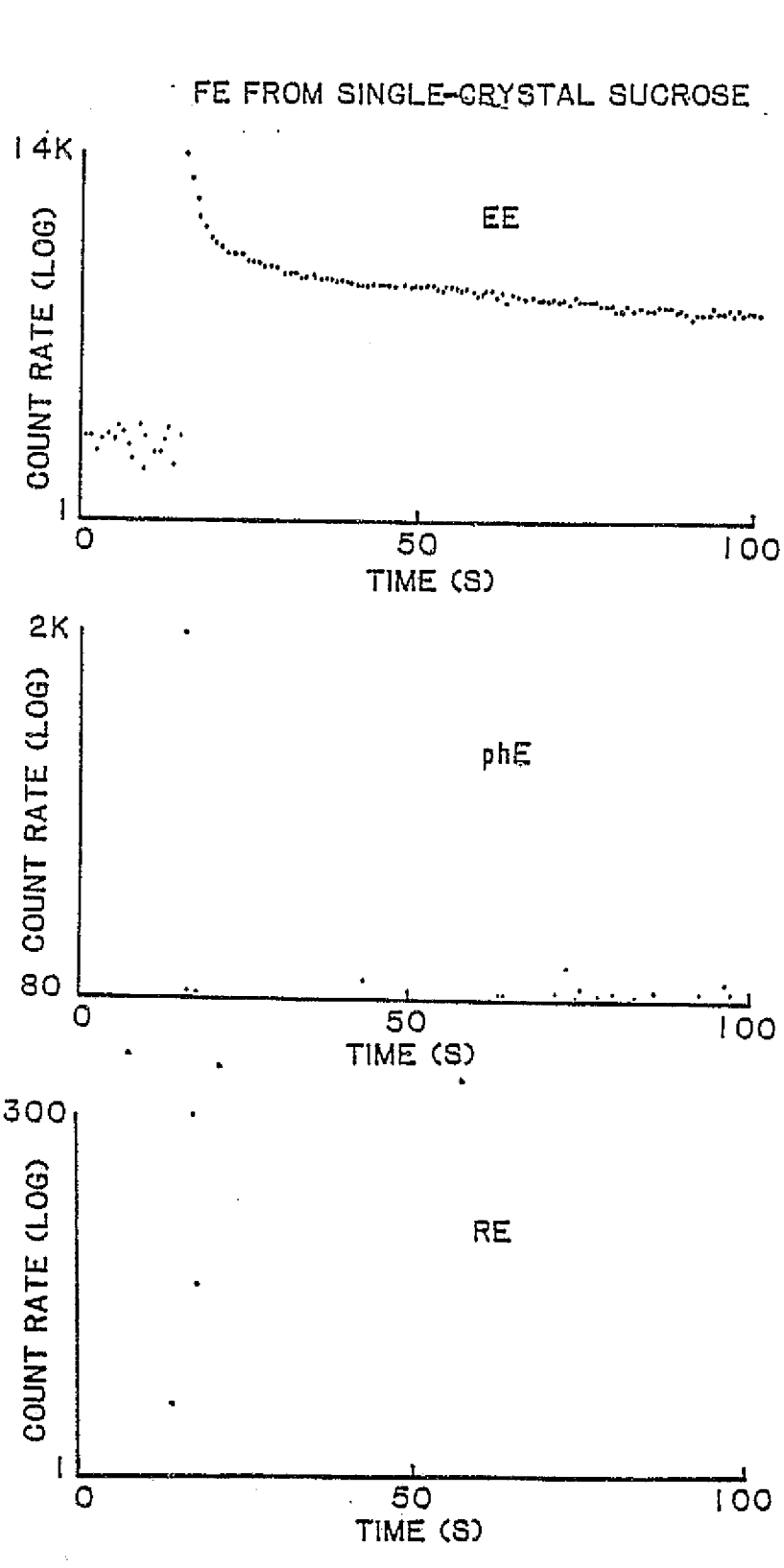

Fig. 3

FE FROM SINGLE-CRYSTAL QUARTZ

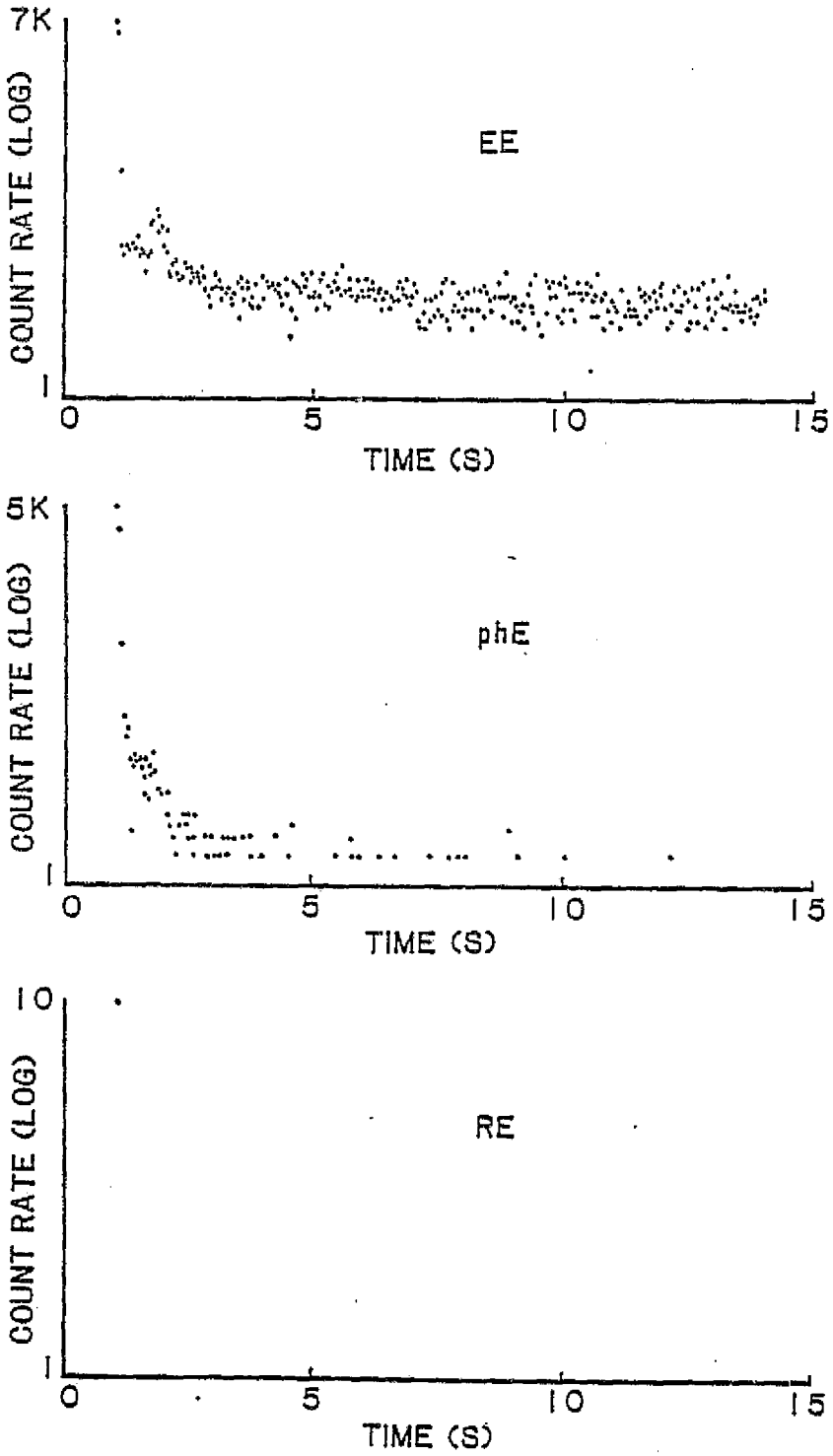

Fig. 4

FE DURING FRACTURE OF
BR FILLED WITH GLASS BEADS

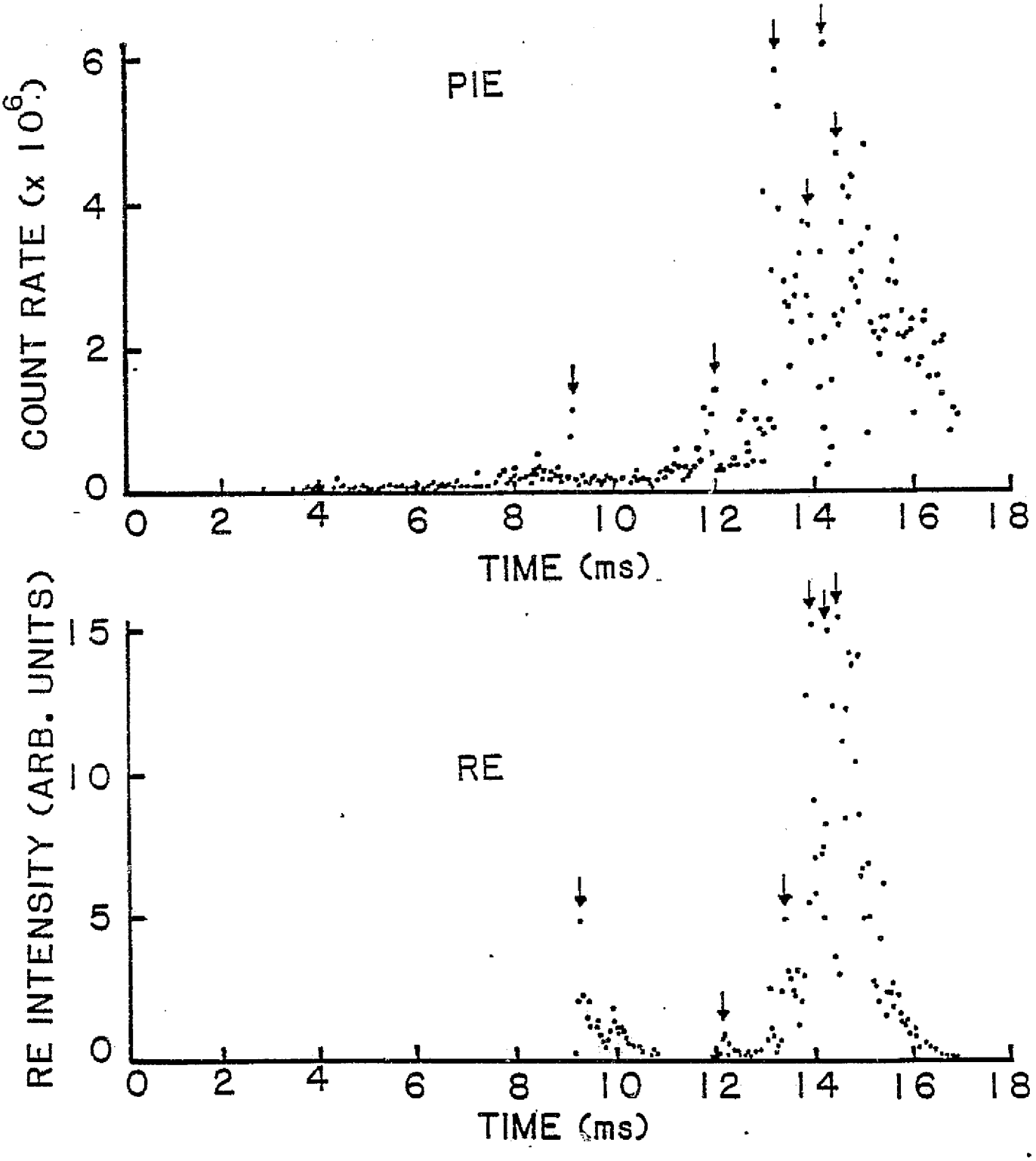

Fig. 5

EFFECT OF ELECTRON BOMBARDMENT OF
POLYBUTADIENE

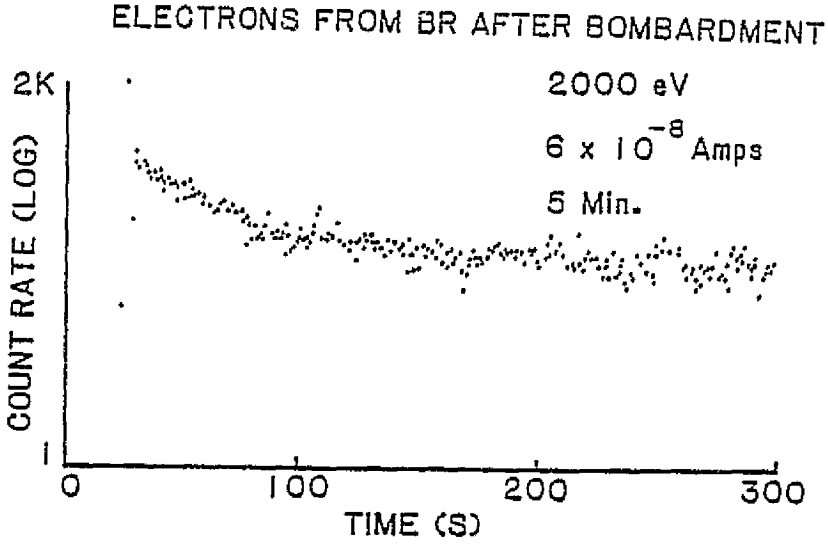

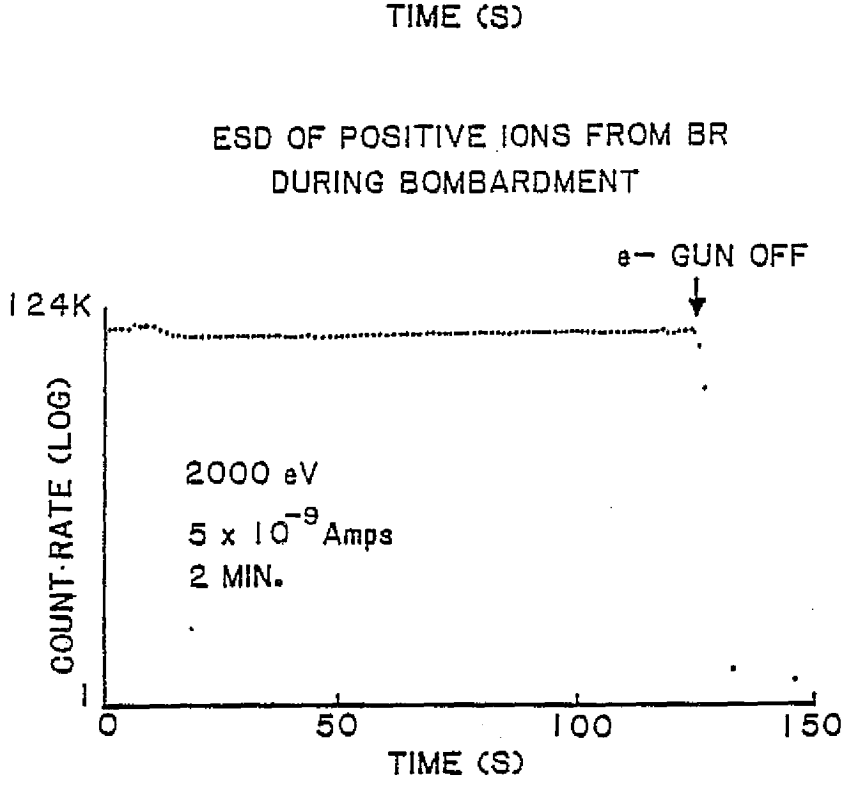

Fig. 6

For Proceedings of Symposium on Polymer Composites, Interfaces, American Chemical Society Meeting, Seattle, WA, 1983.

VI. FRACTO-EMISSION FROM FIBER-REINFORCED AND PARTICULATE FILLED COMPOSITES

J. T. Dickinson, A. Jahan-Latibari, and L. C. Jensen
Department of Physics
Washington State University
Pullman, WA 99164-2814

ABSTRACT

Fracto-emission (FE) is the emission of particles and photons during and following crack propagation. The types of particles we have observed include electrons (EE), positive ions (PIE), and excited and ground state neutral emission (NE). In this paper we present our work on the characterization of the various FE components and measurements relating FE to the fracture events and material properties involved. FE characteristics measured include total emission, time dependence relative to crack propagation, species of neutral and ionic components energy of charged species, and time correlations between pairs of FE components. Experiments on fracture of epoxy, single fibers, fiber/epoxy strands, particulate filled epoxy, and multi-ply fiber/epoxy systems will be presented.

I. INTRODUCTION

When a crack propagates through a material the crack walls are left in a highly excited, non-equilibrium state. For non-metals this departure from equilibrium involves: (1)broken bonds, (2) liberated fragments (e.g. free radicals, atoms, molecules), (3) defects (e.g. in crystals, point defects), (4) charge separation often involving production of charged species, a variety of types of electron traps, and associated electric fields, and (5) a localized rise in temperature. All of these factors represent concentrated energy which can contribute to the ejection or emission of charged particles, neutral particles, and photons from the fracture surfaces. We refer to all forms of such emission accompanying fracture as "fracto-emission" (FE). Our experimental studies of the characteristics of FE from a wide range of materials are presented in references 1-13. A review of our work on FE accompanying adhesive failure can be found in reference 14.

The basic behavior we have observed can be summarized as follows:

(1) Some form of crack propagation appears to be a necessary prerequisite for the occurrence of FE.

(2) FE is a wide-ranging phenomenon. We have observed electron (EE) and positive ion emission (PIE) from all materials tested including inorganic crystalline materials, ceramics, glasses, glassy polymers, filled and unfilled elastomers, fiber-reinforced composites, and molecular crystals.

(3) The few systems we have studied to date emit photons (phE) in air and in vacuum environment.

(4) Interfacial failure between epoxies, polymers, glasses, graphite, and metals produce very intense, long-lasting energetic EE and PIE. This is believed to be due to the production of high concentrations of surface free

radicals and surface charge due to charge separation. The EE and PIE energy distributions which we have measured for these systems are broad, slowly-decreasing functions peaking near 0 eV but extending to beyond 1 keV. These energies are believed to be due to charged particles being accelerated in the presence of the electric fields produced by charge patches on the fracture surface.

(5) Polymeric systems have a strong dependence of EE intensity on crack velocity (V_c). Presumably, this is due to a higher density of free radicals and trapped electrons produced by more primary bond scissions at higher V_c. At lower V_c the polymer has time for slipping and unraveling of chains allowing it to deform and tear with less "damage".

(6) In support of this, more highly cross-linked polymers produce higher intensity and longer-lasting FE (for the same reasons).

(7) The measurements we have made on the mass of PIE produced during fracture indicate that the masses are chain fragments; this implies a sensitivity to where the fracture has occured on an atomic scale.

Our initial work on FE from composites has concentrated on fracture of individual fibers, unfilled resins, and unidirectional fiber/epoxy systems. A few studies of multi-directional fiber/epoxy systems have also been carried out. In addition, we have recently examined FE from particulate-filled epoxy. The results of these studies will be presented here.

II. EXPERIMENTAL PROCEDURE

Details of our experimental procedure are given in references 1-13. In brief, experiments were performed in vacuum at pressures ranging from 10^{-6} to 10^{-3} torr. Our vacuum systems are equipped with devices to stress

samples in various ways including tension, flex, and compression, while measuring stress and/or strain. The detectors used for charged particles are channeltron electron multipliers (CEM) which produce fast (10ns) pulses with approximately 90% absolute detection efficiency for electrons and nearly 100% efficiency for positive ions. The gains of the CEM's used were typically 10^6 - 10^8 electrons/incident particle. The detectors were positioned 1 - 4 cm away from the sample with a bias voltage on the front cone of the CEM to attract the charged particles of interest. Background noise counts ranged from 1 to 10 counts/second. Standard nuclear physics data aquisition techniques were employed to count and store pulses, normally as functions of time. The time scales of interest are submicrosecond to several second intervals, which we can easily cover with commercial electronics. Single fibers and epoxy-filament strands were tested in tension at a rate of 1% per second. Fiber samples consisted of 5-20 fibers adhesively bonded to Al sheet metal shaped to fit into clamps in the vacuum system. To reduce the probability of fiber pull-out, the fibers were stretched across a sharp Al edge, where approximately 90% of them fractured.

Kevlar, E-glass, and S-glass epoxy-strands and unidirectional graphite-epoxy composite made from Union Carbide Thornel 300 graphite fibers and NARMCO 5208 epoxy resin were also fractured in tension. A sharp notch was made in the center of the tension sample to control the fracture initiation.

Graphite-epoxy composites made from Union-Carbide Thornel 300 fibers and various NARMCO epoxy resins were tested in flex as well. The fiber directions in these composites were (0), ($\pm$45) and (0,90,90,0) degree to the long axis. Samples were tested with a span-to-depth ratio of 30:1 and strain rate of 0.064 mm/sec. Acoustic emission (AE) and EE were detected from graphite-epoxy composite fractured in flex. AE was detected with a PZT

transducer with a resonant frequency of 175 KHz. The bursts were typically 500 μs in duration. The filtered and amplified signal was fed into a discriminator to eliminate background noise, and the resulting pulses were counted on a multi-channel scaler. Thus the count rate displayed is determined by both the number and size of AE bursts (the number of "rings" that trigger the discriminator). To reduce the influence of mechanical AE in our experiments the mechanical supports were covered with teflon tape. Fracture of a uniform material (PMMA), which will have no interlaminar shear or delamination, shows no prefracture AE in our system. Fig. 1 shows schematically the electron multipler and AE transducer arrangement which simultaneously detects AE and EE from the sample. Load and deflection were also measured.

Another composite structure we have investigated recently is a particulate-filled epoxy. The epoxy is EPON 828 (Z-hardener) filled with irregularly shaped alumina particles with an average diameter of approximately 10 μm. This brittle material was broken in flex.

III. RESULTS AND DISCUSSION

Filament-Epoxy Strands: An early observation we made involving adhesive failure and its effect on charged particle emission concerned the fracture of composites. Starting with the constituents of a composite, the EE time distributions of the fracture of individual 10-20 μm filaments of Kevlar^{TM}, Thornel 300 graphite, E-glass, and S-glass, as measured with a CEM 1 cm from the sample, are shown in Fig. 2. Also shown is the EE from the fracture of unfilled DER 332/T403, a bisphenol-A type resin. With the exception of Kevlar filaments, repeated experiments showed no evidence of a measurable rise to the peak emission. The brittle fibers with small cross section break on a

microsecond time scale. The peak emission occurs during fracture and decays rapidly away, typically in 10 - 100 μs as shown in Fig. 2.

When these fibers are placed in the epoxy resin and fractured, the results are significantly different. Fig. 3 shows the EE and PIE resulting from the failure of a strand containing Kevlar fibers in DOW DER 332 epoxy. These curves were taken simultaneously with two detectors. In general, EE exceeds PIE in terms of total emission by 10-40%; in Fig. 3 PIE has been normalized to the EE at a single point. On the time scale shown, the time required for fracture was less than one channel. Thus, the signal rises from a noise count of 0.1 to 10/sec to peaks of 10^4-10^5 counts/sec. Note that in this case the decay from the peak lasts for many seconds; intense emitters such as these can give detectable emission for as long as 2 hours after fracture. Also note that the decay kinetics for both EE and PIE are essentially identical, suggesting that a common rate-limiting step is shared by the two types of emission.

Examination with an SEM of the fracture surface on a number of systems involving adhesive failure or delamination indicate that the production of interfaces is responsible for the considerable differences between Fig. 2 and Fig. 3. This feature of intense, long lasting emission may serve as a measure of the extent of delamination that has occured. In support of this, in Fig. 4a and 4b we compare the EE for two types of epoxy strands made from 20 μm diameter E-glass filaments and 10 μm S-glass filaments embedded in DOW DER 332 epoxy (Note the different time scales for the two different materials). Examination under the SEM shows that there is considerably more delamination and separation of the filaments in the case of E-glass than for S-glass epoxy strands, which apparently results in considerably higher count rates and longer-lasting emission. By far the predominant emission is coming from the

surfaces created by the separation of the filaments from the matrix.

The results of experiments on unidirectional graphite-epoxy composites (Thornel 300/5208) are shown in Fig. 6. The samples were 0.25 mm thick and 2.4 mm wide. The EE and PIE were measured from two separate samples. The resulting emission plotted on a log scale shows the rapid rise during fracture and slow decay following fracture. Examination of the fracture surfaces shows extensive delamination and interfacial-like failure, consistent with the results on DOW DER 332/Kevlar strands.

Energy Distributions: Because the EE and PIE from systems involving interfacial failure frequently was intense and long-lasting, we were able to take measurements of the energy distributions, n(E), using retarding potential analysis. The curves in Fig. 6 represent n(E)dE, where dE is 2 eV, plotted on a log scale and normalized to unity at the peak. Both curves are very similar (within our experimental error, they are identical), showing a peak near 0 eV and a significant number of higher energy particles in the tail. It is well known that charge separation is a common occurrence with adhesive failure and can leave the surfaces in a highly charged state. Thus the probable cause of the high energy particles is the release of the charges in physical proximity of charge patches of the same sign, yielding an acceleration of the particles to the observed energies.

Preliminary experiments involving fracture of the filaments and neat resin alone do not seem to yield emission at such high energies. Thus we appear to have a distinct indicator of interfacial failure in a composite system:

a) intense, long-lasting EE and PIE

b) the presence of high energy EE and PIE.

Retarding grids could easily reject the low energy particles and thus obtain a

signal which is entirely due to interfacial failure. Proper steps to quantify these measurements could allow a precise determination of the degree of delamination/interfacial failure that has occured during a fracture event.

TOF Measurements of PIE Mass from Fracture of Filaments: To determine the masses of the positive ions emitted from Kevlar and E-glass fibers we have devised a time-of-flight (TOF) technique (14) (shown schematically in Fig. 7). The fibers, upon fracture, emit bursts of EE and PIE simultaneously, as determined by a number of experiments using two detectors close to the sample. By triggering a multichannel analyzer (MCA) with the EE burst we can record the time of arrival of the corresponding PIE burst down a 25 cm drift tube. From the leading edge of these TOF distributions one can measure a TOF corresponding to the fastest (presumably the lightest) positive ions emitted.

Fig. 8 shows the leading edges of TOF distributions obtained for PIE from Kevlar and E-glass fibers for a 500 V drift tube potential (-V). Five to ten curves like these were acquired for each of these four values of -V and an average time obtained. The average time at each voltage was plotted vs the inverse square root of the potential and the slopes of these lines were used to calculate M/q. M/q values of 60 ± 20 a.m.u and 48 ± 12 a.m.u. were obtained for Kevlar and E-glass, respectively.

Although the uncertainties in these values of M/q are relatively large, we emphasize that the M/q of the PIE accompanying fracture of materials has previously been totally unknown. The technique we have employed here favors the detection of the lightest masses if more than one mass is emitted. Nevertheless we have some sensitivity to the presence of heavier masses which should show up as a shoulder on the leading edge of the TOF distribution at longer times. Careful examination of a number of TOF distributions both for

Kevlar and E-glass show no clear evidence of heavier masses. Therefore our present results indicate that the PIE accompanying fracture of these materials consists of relatively light ions.

For each material our uncertainties do not allow a unique value of mass to be assigned to the observed PIE and therefore a number of candidates have been examined. For Kevlar, we can rule out absorbed H_2O and ions of common background and atmospheric gases. If we assume q=e, the PIE mass from Kevlar is considerably smaller than a monomer. Likely candidates are:

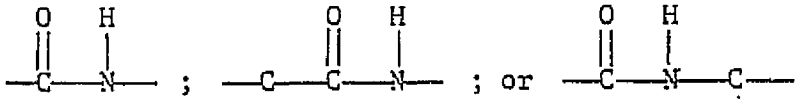

all of which could be produced by chain bond cleavage. For E-glass, if we assume q=e, we can rule out H_2O^+ and O_2. Fragments of the constituent atoms/molecules of E-glass which are possible candidates include Ca^+, K^+, and possibly SiO^+. Reference 11 discusses a TOF technique that takes advantage of the coincidence between individual electrons and positive ions that we have observed. This method has been applied to the measurement of PIE masses from the fracture of filled polybutadiene, an elastomer. We also applied the method to Kevlar-epoxy strands.

Fig. 9 is the resulting TOF curve from fracture of a Kevlar-epoxy strand for the same drift tube length of 25 cm and a tube voltage of -2kV. The peaks over the time interval 1 to 5 μs are due to heavier ions; we are still in the process of identifying them. The large feature in the first channel (0-0.25

μs) is also a positive ion (it can be shifted slightly by changing the voltage on the tube). For reasonable initial kinetic energies (less than a few keV) the only M capable of reaching the detector that fast is mass 1 or 2, i.e. hydrogen. We conclude, therefore, H^+ or H_2^+ is a predominant component of the PIE from this particular material. Of course both the epoxy resin and the Kevlar filaments contain abundant quantities of hydrogen.

AE and EE from Flexural Testing of Fiber-Reinforced Composites: To further explore the type of fracture events in composites which lead to FE, we simultaneously examined the AE and EE accompanying flexural failure. Figs. 10 thru 12 show the results of AE and EE measurement from $(0)_{16}$, $(\pm 45)_{16}$, and $(0,90,90,0)_{16}$ graphite-epoxy composite. Load vs. deflection curves are also included in figures 10 thru 12 to better demonstrate the dependence of AE and EE on the deformation and failure of composite materials. In general the AE data obtained from these experiments can be characterized as follows: first, an initial rapid rise from zero due to the initial load applied to the specimen; second, the steady build up of the AE count rate prior to failure. Finally, a large burst followed by a drop in AE count rate at catastrophic failure.

Concerning AE only, our result differs somewhat from those of Barnly and Parry (15). Barnly and Parry observed no acoustic activity prior to fracture for unidirectional fiber glass-epoxy composite notched flex samples. In their experiment, the onset of failure and large load drop was indicated by the onset of AE. However, their result on cross-ply (0/90) material showed the AE build up immediately following the application of load. Fitz-Randolph et.al. (15) have shown the steady increase of AE with deflection for unidirectional boron-epoxy composites.

Composite materials generally exhibit a variety of failure modes including

matrix crazing or microcracking, debonding, fiber failures resulting from statistically distibuted flaw strength, delamination, and void growth (17). Some of these events, prior to failure, will be clearly detectable in both EE and AE.

The basic requirement for detecting fracture events with FE is that the newly created fracture surfaces are in some manner in communication with the vacuum so that the particles can escape from the sample and be detected. Thus, the existence or lack of correlations between AE and FE can provide information on the mechanisms leading up to failure.

For example, Fig. 10 shows the AE build-up in an $(0)_{16}$ graphite/epoxy system at the early stages of loading. Because of the statistical nature of the fiber strength, some may fracture at a very low stress in tension, which will also contribute to the AE count rate. Shear and delamination are the dominant failure mechanisms in this instance; the main souce of AE is the interlaminar shear. Loose fibers at the edges may break at any time during loading and produce both AE and EE bursts simultaneously. As the loading advances, interlaminar shear and internal delamination will lead to AE. Matrix cracking in the tension side of the sample and the separation of tiny bundles of fibers will all contribute to simultaneous AE and EE. Thus, the slow build-up of EE prior to failure is attributed to small microcracks formed on the surface. The bursts of EE prior to failure are considered to be due to "larger" events such as edge cracking or bundles fracturing on the front surface. Finally, the test specimen fails catastrophically (where the load drops), accompanied by large bursts of AE and EE occurring together. One can frequently see several plys failing successively.

Even though some of the composite failure mechanisms described above will apply to angle ply laminates, transverse cracking and interfacial failure will

predominate. When reinforcement fibers are at ±45 degree to the long axis, interfacial failure is the main failure mechanism. This is clearly seen in Fig. 11 from simultaneous large bursts of AE and EE. Interlaminar shear contributes to continous AE build up. One interesting feature of AE and EE data from (0/90/90/0) degree samples is the AE build up without any appearance of EE prior to failure. Large interlaminar shear deformation and failure will occur in 90 degree (interior) laminates prior to the failure of zero degree (exterior) laminates (Fig. 12). These events apparently cannot be detected using EE due to their being internal to the sample.

The results of these experiments indicate that it is possible to detect microfractures, such as microscopic separation of tiny bundles of fibers, interfacial failure and matrix crazing, in fiber-reinforced composites using EE. Even though the EE technique is not able to detect internal failure such as interlaminar shear failure, it will provide evidence of failure at early stages of fracture. Also, it clarifies the source of AE as a function of strain by the presence or absence of AE-EE correlations. Finally, comparisons of the techiniques tell precisely the onset times for internal and external failure.

EE from Particulate-Filled Epoxy: Another form of reinforced plastics which have gained popularity are the particulate filled plastics. Particles of silica or alumina are incorporated into plastics primarily because of their low cost. In addition, some material properties may improve to some extent. In our studies we examined EPON 828 epoxy (Z-hardener) filled with irregularly shaped alumina particles. This material is quite strong and brittle so we fractured most of the samples in a three-point flexure mode. The cross-section of the sample was 2 mm x .6 mm. A typical EE curve plotted on a log scale is shown in Fig. 13, where t = 0 corresponds to the instant of

failure. The material for this emission curve is filled at an Al_2O_3/epoxy ratio (α) of 3 to 1 by weight.

The emission intensity is strongly influenced by the concentration of filler particles. Taking just the first channel (0.8 seconds per channel) count as a measure of the initial EE count rate vs. the Al_2O_3/epoxy ratio, one sees this dependence in Fig. 14. The total emission (measured over several hundred seconds) follows basically the same curve. Compared to the unfilled material ($\alpha = 0$) the EE intensity rises rapidly as a increases, and peaks near $\alpha = 1$. This is followed by a slower decline.

These results are preliminary, and we are not entirely sure why the EE. intensity depends on a in this fashion. Optical inspection of the fracture surface indicates that alumina particles are indeed being exposed, although SEM micrographs are far less convincing so we are not at this point sure of the degree of interfacial failure that is occurring. Secondly, as α increases, the mechanical parameters such as fracture energy, surface energy, and the degree of interfacial failure are bound to change. We are obviously interested in correlating these mechanical properties with the resulting EE.

Photon-Emission Measurement from Filament-Epoxy Strands: Photon emission (phE) accompanying fracture appears to be of a different character. We have performed in air a number of experiments on the phE from epoxy strands of filaments with a strand cross-section of 0.5 mm^2. Fig. 15 shows the visible light emission accompanying the straining and failure of epoxy strands of Kevlar, E-glass, and graphite. Several show phE prior to failure, possibly due to crack formation on a surface visible to the photomultiplier, or to chemiluminescence as observed by George and Pinkerton (18), and Fanter and Levy (19). The decay that we observe for the phE following fracture is within the time constant of the electrometer used to measure the photon detector current.

Although the cause of the major burst of phE during fracture is unknown, we suspect, as with many cases of triboluminescence, that breakdown is occuring in the crack tip due to the high potentials produced by charge separation. This will be particularly intense at instances when delamination and adhesive failure are occuring. Further experiments need to be carried out to confirm this.

PhE was also measured during "T" peel tests of two-ply Kevlar-epoxy panels. The entrance to the photomultiplier was approximately 2 cm from the "crack", and directed toward it. PhE was observed only during separation of the plys and decayed immediately upon release of the stress. For a constant area of new fracture surface (5 cm^2), the intensity of phE per unit area of fracture surface was found to depend strongly on the crack velocity, defined as the linear rate of the creation of new surface (cm/s). Fig. 16 shows the phE for a typical delamination. Fig. 17 shows this dependence where the ordinate represents the area under the emission curves for various velocities. The light intensity tends to increase for more rapid separation of the two surfaces, with a saturation occurring at a velocity of 10^{-1} cm/s.

IV. CONCLUSIONS

We have tried to show a wide variety of FE results on a number of systems involving adhesive failure at interfaces and indicate some of the parameters that are influencing this emission. The need for careful studies of the physics and chemistry of these phenomena is obvious. The usefulness of FE as a tool for NDT or for investigation of failure mechanisms require a broad based attack combining fracture mechanics, materials science, and fundamental fracto-emission studies on materials of mutual interest. Potential areas of

usefulness for FE in the study of composite failure include the following:

1. As a probe of crack growth on an extremely wide range of time scales. These need not be catastrophic fracture and might involve crazing, micro-cracking, linking of microcracks, and other pre-failure events.

2. The energies of the FE components may serve as a measure of the density of the charge distributions created on the fracture surface and relate to debonding parameters between the fiber and resin.

3. FE may serve as a way to measure the surface temperature at the crack tip by careful modeling of the emission curves at short times after fracture. Our modeling to date has required an elevated temperature of fracture that decays quickly away.

4. FE may serve as a means of measuring instantaneous crack velocity. Certainly the onset of crack formation and the onset and duration of dynamic crack growth can be readily measured.

5. FE may serve as a probe of the locus of fracture in composite materials and in illuminating failure mechanisms.

6. FE may serve as an NDT tool, perhaps in conjuction with acoustic emission. FE would be particularly useful when sensitivity to events near the surface is desired.

7. FE may be related in important ways to fracture mechanics parameters such as surface energy, fracture strength, or fracture toughness. If reliable connections would be made to such parameters, FE might be used to measure them.

V. ACKNOWLEDGEMENTS

First we wish to thank our Washington State University colleague Ed Donaldson for his helpful discussions and contributions. We also wish to thank those people who have contributed specimens used in these studies, particularly R.L. Moore, Lawrence Livermore Laboratory, for samples of filaments and fiber/epoxy strands. We are also apreciative of interest and advice from O. Ishai, A. Gray, and L.C. Clements of NASA-Ames Research Center, and W.D. Williams, Sandia National Laboratories.

This work was supported by the Office of Naval Research contract N0014-80-C-0213, Sandia National Laboratories, Nasa-Ames Research Center, and a grant from the M.J.Murdock Charitable Trust.

REFERENCES

1. J. T. Dickinson, P. F. Braunlich, L. Larson, and A. Marceau, Appl. Surf. Sci. 1, 515 (1978).

2. D. L. Doering, T. Oda, J. T. Dickinson, and P. F. Braunlich, Appl. Surf. Sci. 3, 196 (1979).

3. L. A. Larson, J. T. Dickinson, P. F. Braunlich, and D. B. Snyder, J. Vac. Sci. Technol. 16, 590 (1979).

4. J. T. Dickinson, D. B. Snyder, And E. E. Donaldson, J. Vac. Sci. Technol. 17, 429 (1981).

5. J. T. Dickinson, D. B. Snyder, and E. E. Donaldson, Thin Solid Films 72, 225 (1980).

6. J. T. Dickinson, E. E. Donaldson, and D. B. Snyder, J. Vac. Sci. Technol. 18, 238 (1981).

7. J. T. Dickinson, E. E. Donaldson, and M. K. Park, J. Mat. Sci 16, 2897 (1981).

8. J. T. Dickinson and L. C. Jensen, J. Polymer Sci. Polymer Physics Ed. 20, 1925 (1982).

9. J. T. Dickinson, M. K. Park, E. E. Donaldson, and L. C. Jensen, J. Vac. Sci. Technol. 20, 436 (1982).

10. J. T. Dickinson, L. C. Jensen, and M. K. Park, J. Mat. Sci., 17, 3173 (1982).

11. J. T. Dickinson, L. C. Jensen, and M. K. Park, Appl. Phys. Letters 41, 443 (1982).

12. J. T. Dickinson, L. C. Jensen, and M. K. Park, Appl. Phys. Letters 41, 827 (1982).

13. H. Miles and J. T. Dickinson, Appl. Phys. Letters 41, 924 (1982).

14. J. T. Dickinson, "Fracto-Emission Accompanying Adhesive Failure," To Appear in Proceedings of the Symposium on Recent Developments in Adhesive Chemistry, ACS seattle, 1983.

15. J. T. Barnby and T. Parry, J. Phys. D: Appl. Phys. 9, 1919 (1976).

16. J. Fitz-Randolph, D. C. Phillips, P. W. R. Beaumont, and A. S. Tetelman, J. Mat. Sci. 7, 289 (1972).

17. C. K. H. Dharan, J. Mat. Eng. Tech., 100, 233 (1972).

18. G. A. George and D. M. Pinkerton, Proceedings of a Critical Review of Characterization of Composites, June 8-10, 1981, Massachusetts Institute of Technology, (Office of Naval Research, 666 Summer St. Boston, MA, 1981).

18. D. L. Fanter and R. L. Levy, in ACS Symposium Series No. 95, Durability of Macromolecular Materials, R. K. Iby, Editor, pp: 211 (American Chemical Society, Washington D.C. 1979).

FIGURE CAPTIONS

Fig. 1. Schematic diagram of experimental arrangement for EE, AE, and load measurements on composite materials in flex.

Fig. 2. The time distribution of EE due to the fracture of graphite, E-glass, Kevlar filaments and bulk epoxy (DOW DER 332/T304). Note the fast time scale.

Fig. 3. EE and PIE from the fracture of Kevlar/Epoxy strands.

Fig. 4. EE during and following fracture of a) E-Glass and b) S-Glass-epoxy strands. Note the different time scales.

Fig. 5. EE and PIE from the tensile failure of unidirectional graphite-epoxy composite (Union Carbide Thornel 300 graphite fiber and NARMCO 5208 epoxy resin).

Fig. 6. Energy distribution on a log scale for EE and PIE from Kevlar/Epoxy strands.

Fig. 7. The experimental arrangement for use in the time-of-flight technique. The distances are $d_1 = d_3 = 1$ cm, $d_2 = 25$ cm.

Fig. 8. The leading edge of the PIE TOF distribution for E-Glass and Kevlar fibers.

Fig. 9. The TOF for PIE from the fracture of Kevlar/Epoxy strands. The major peak near 0 μs is attributed to H^+ or H_2^+.

Fig. 10. The EE, AE, and load accompanying the flexural straining of 16 layer, unidirectional graphite-epoxy composite. (Union Carbide Thornel 300 graphite fiber and NARMCO 5209 epoxy resin.)

Fig. 11. The EE, AE, and load accompanying the flexural straining of 16 layer (±45°), graphite-epoxy composite. (Union Carbide Thornel 300 and NARMCO 5208 epoxy resin.)

Fig. 12. The EE, AE, and load accompanying the flexural straining of 16 layer, cross ply (0, 90, 90, 0)° graphite-epoxy composite. (Union Carbide Thornel 300 graphite fiber and NARMCO 934 epoxy resin.)

Fig. 13. Typical EE curve plotted on a log scale from the fracture of an alumina particle filled epoxy.

Fig. 14. Peak EE as a function of the Al_2O_3/epoxy ratio, α.

Fig. 15. Photon-emission accompanying the fracture of Kevlar, E-Glass, and Graphite epoxy strands.

Fig. 16. Photon-emission from the delamination of a Kevlar/Epoxy composite.

Fig. 17. Photon-emission from Kevlar/Epoxy delamination as a function of various peel velocities.

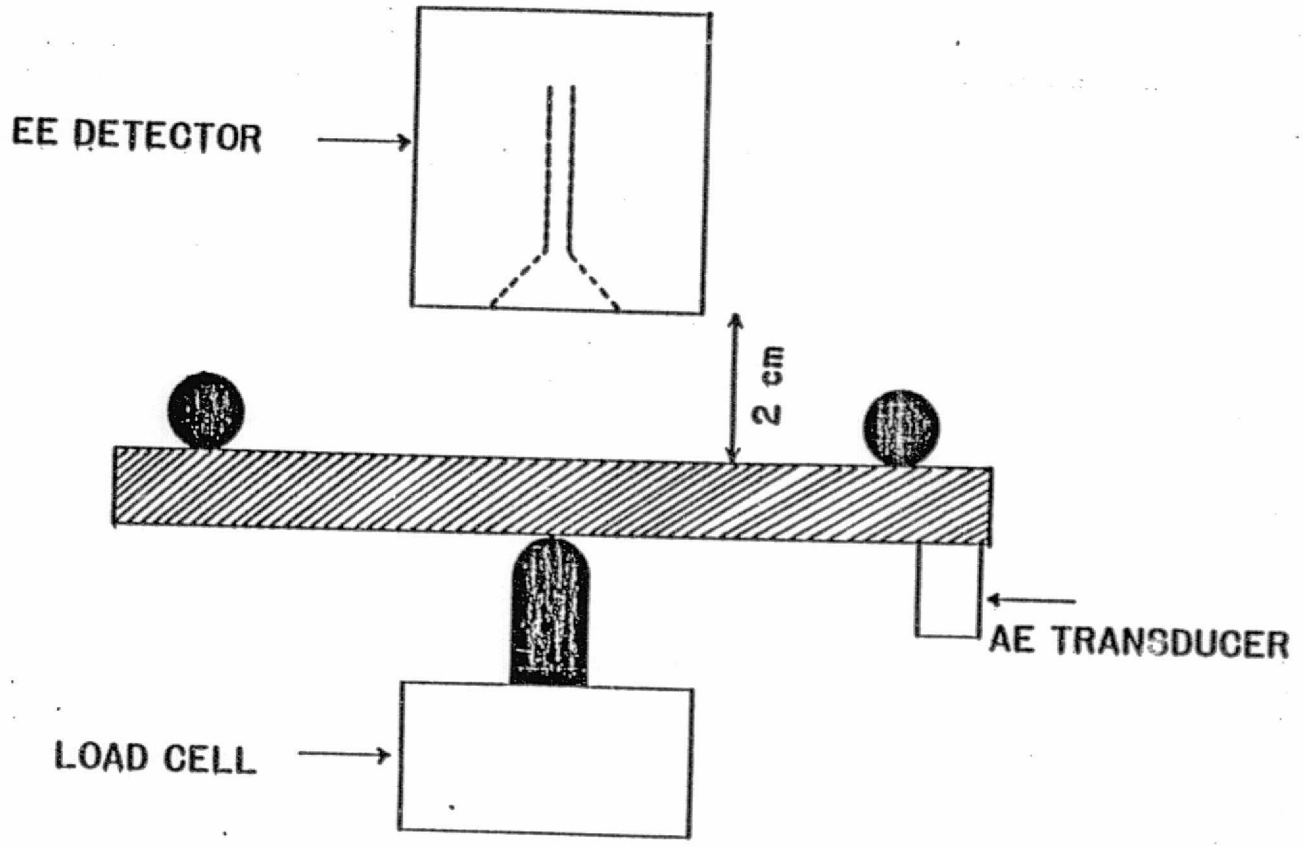

Fig. 1

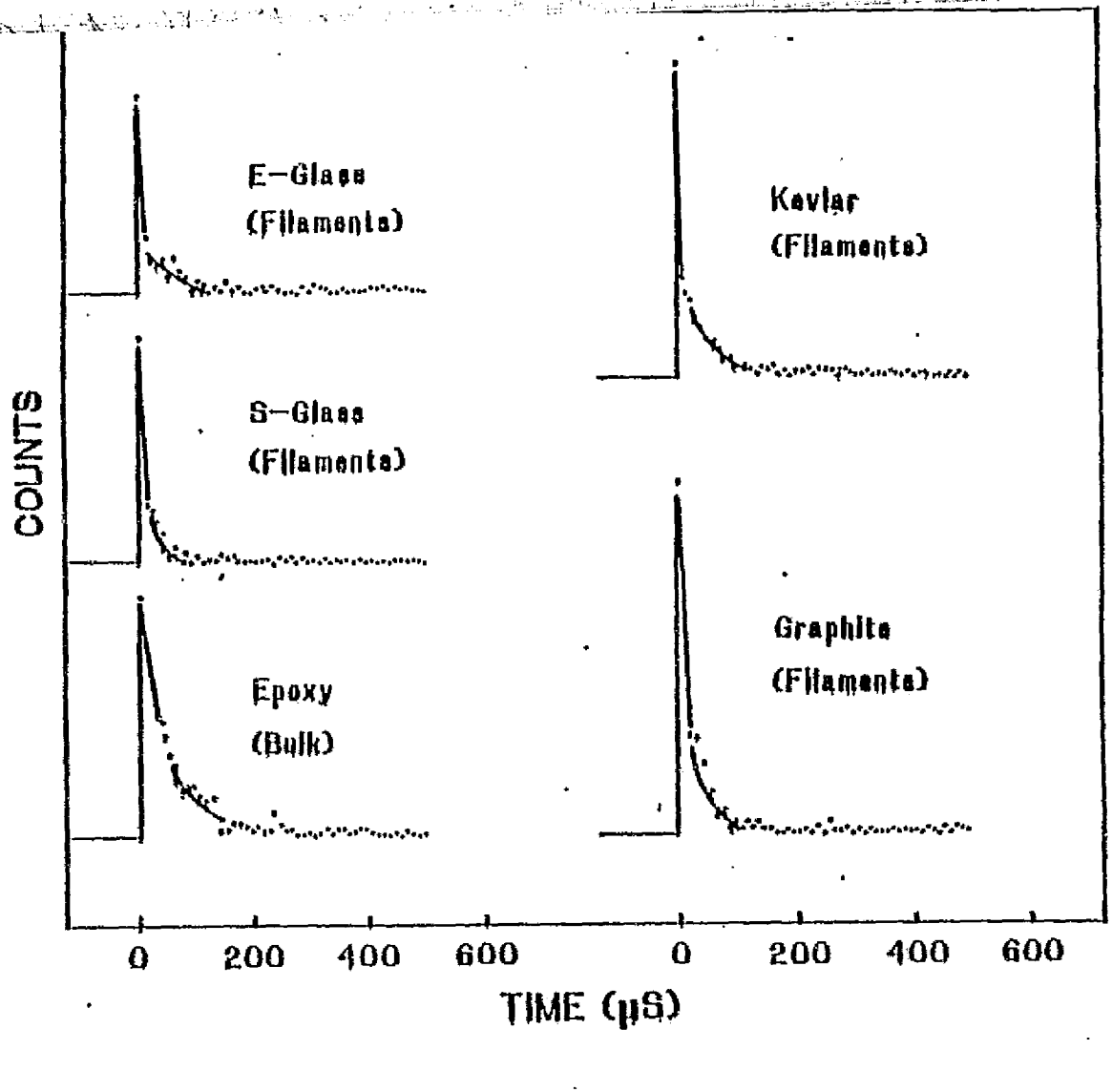

Fig. 2

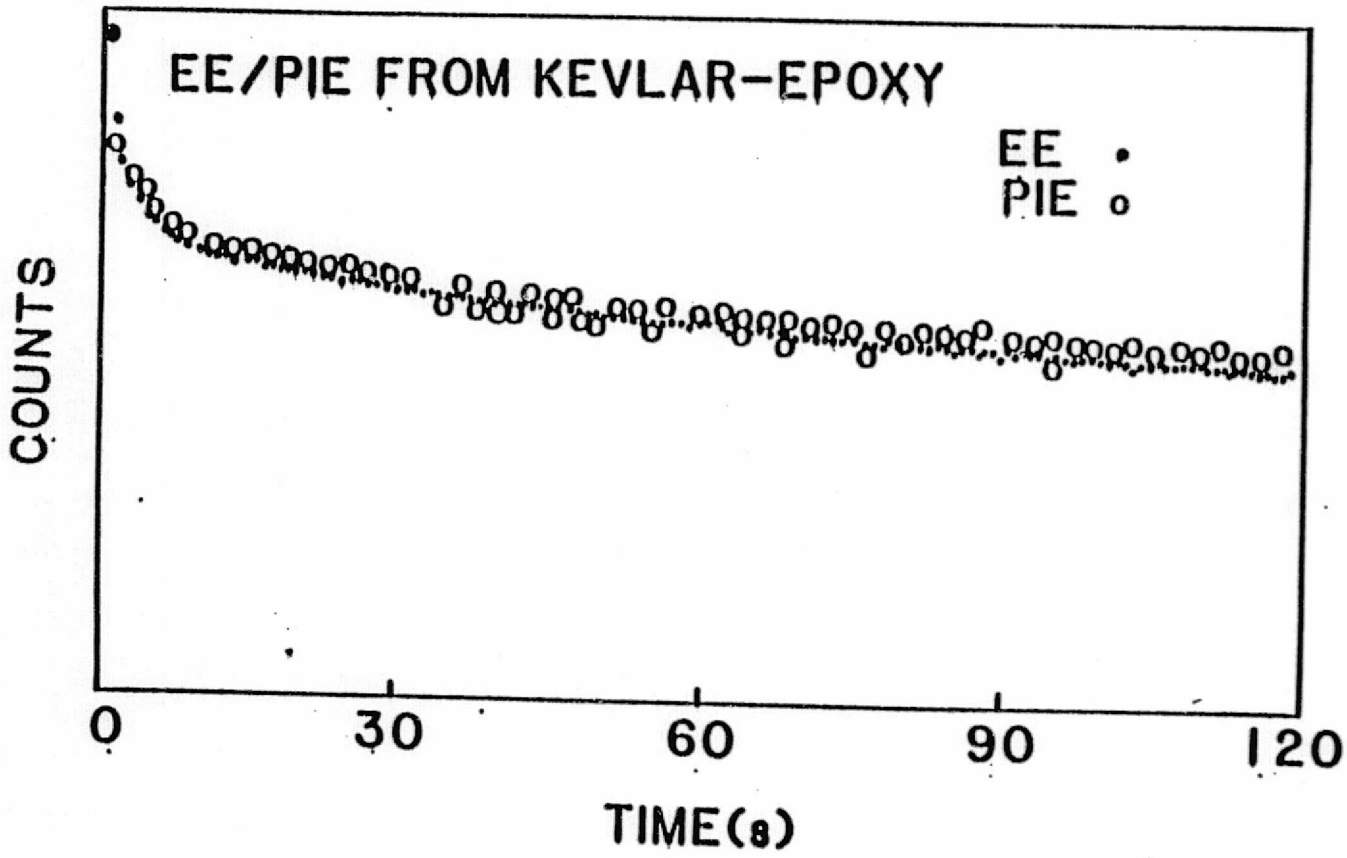

Fig. 3

ELECTRON EMISSION FROM FRACTURE OF FIBRE-REINFORCED EPOXY UNDER TENSILE STRAIN

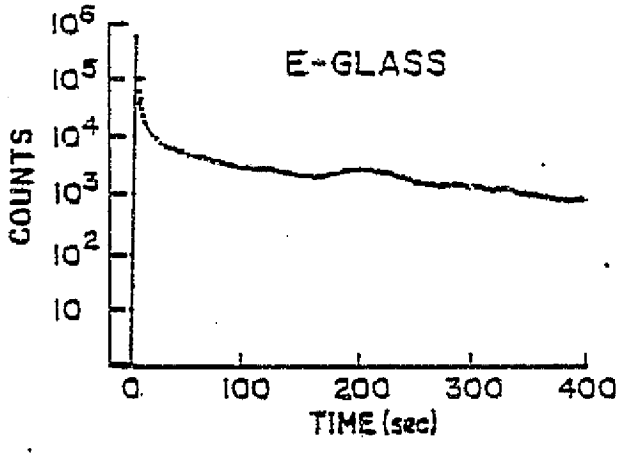

(a)

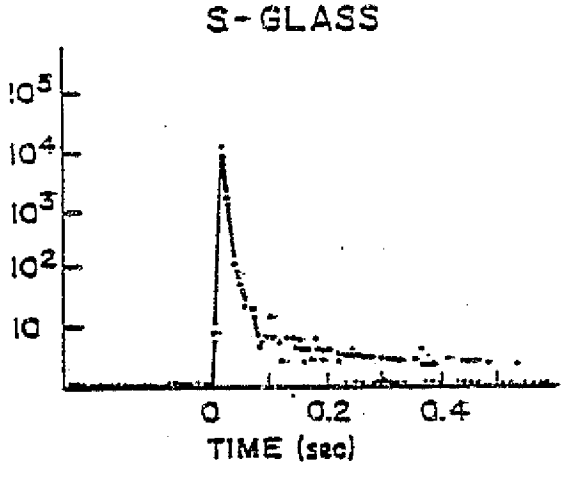

(b)

Fig. 4

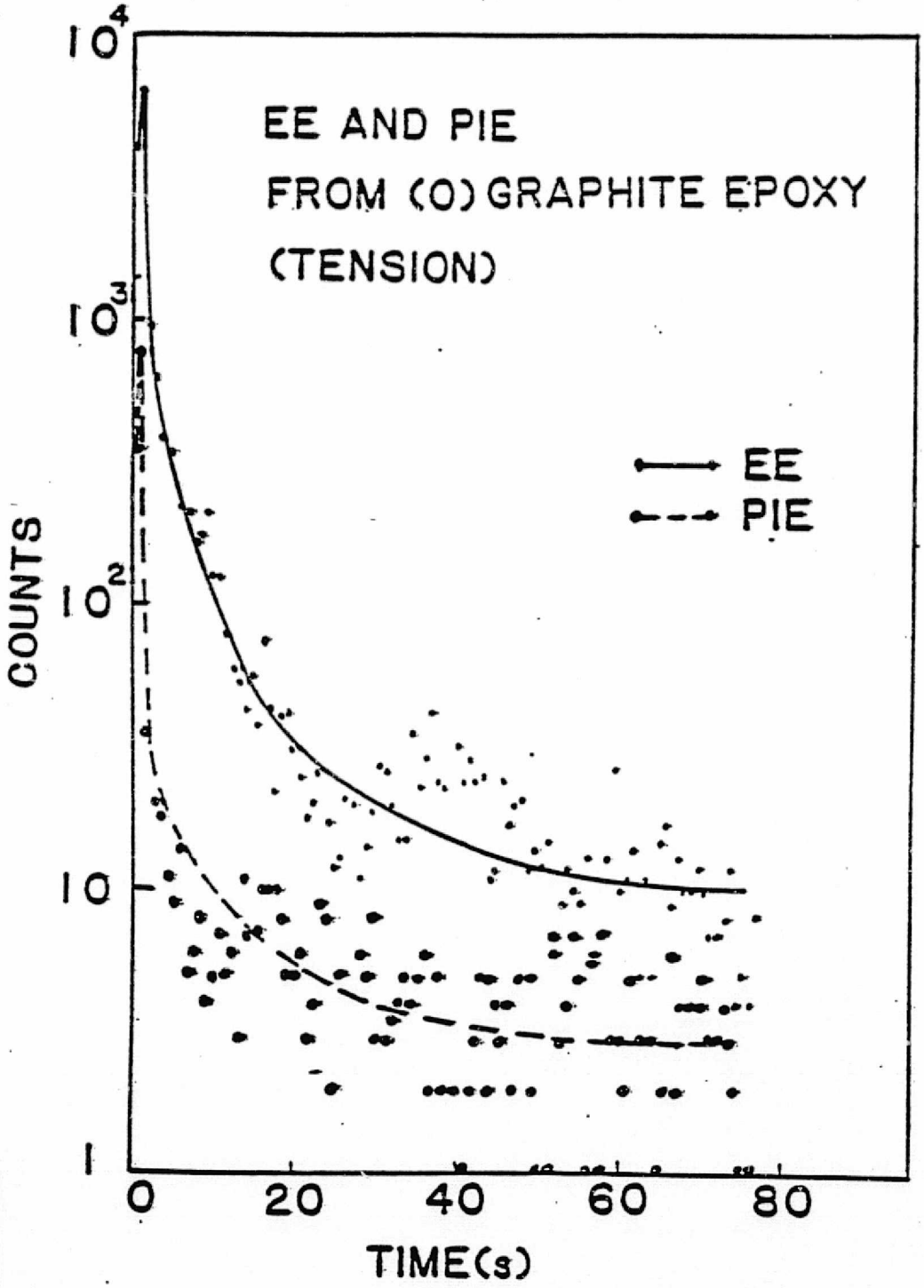

Fig. 5

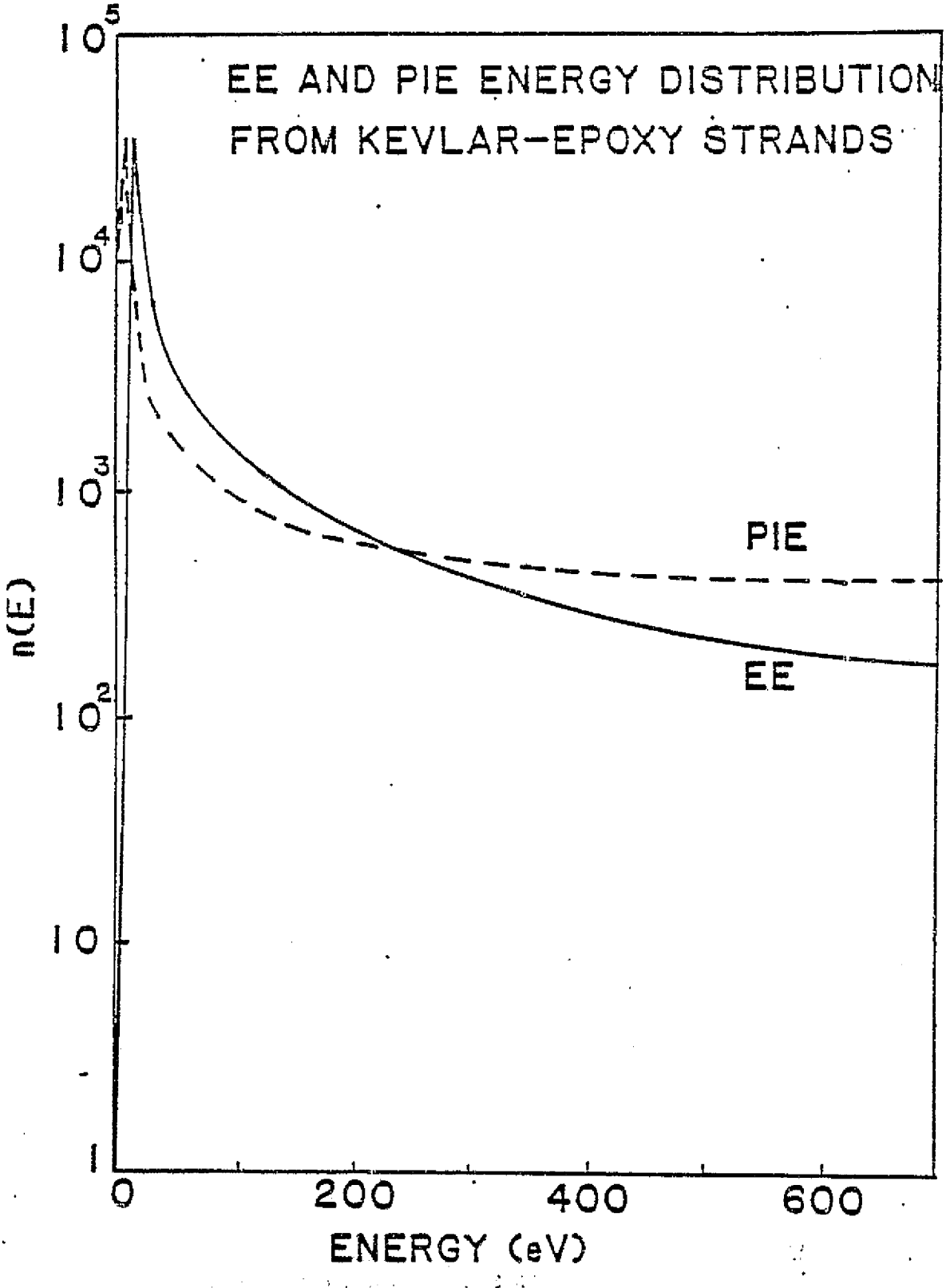

Fig 6

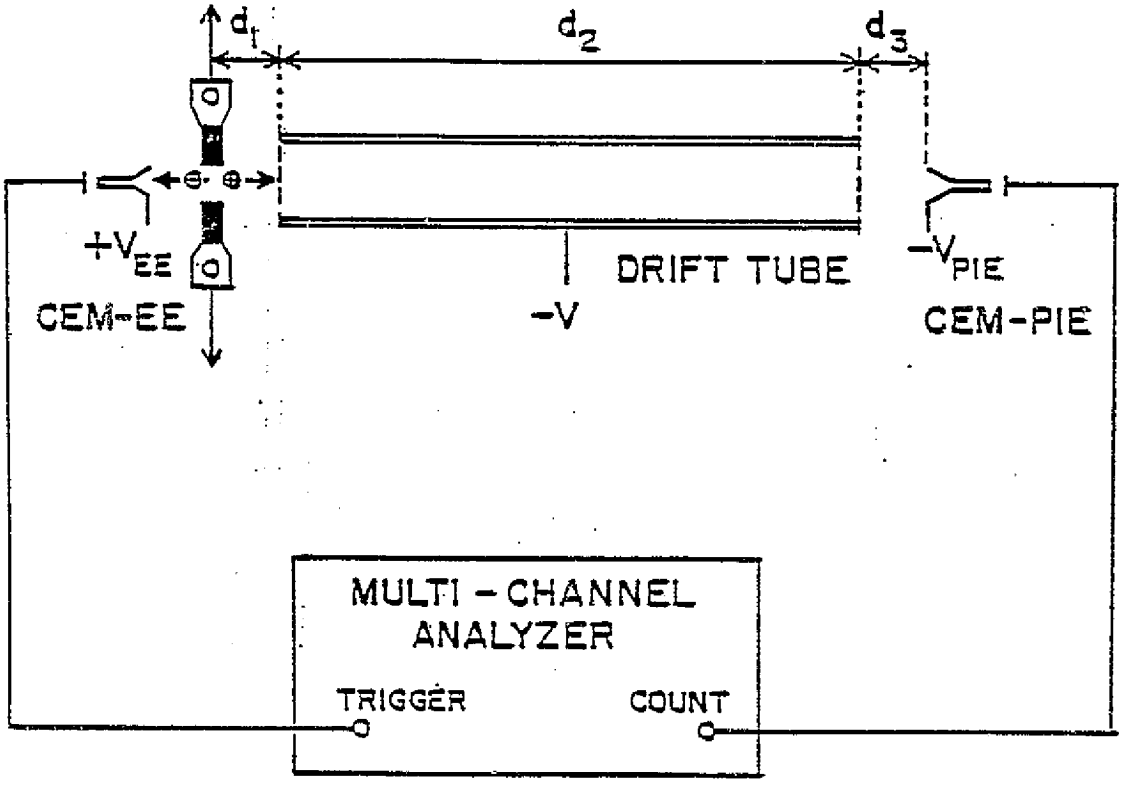

Fig. 7

ORIGINAL PAGE IS
OF POOR QUALITY

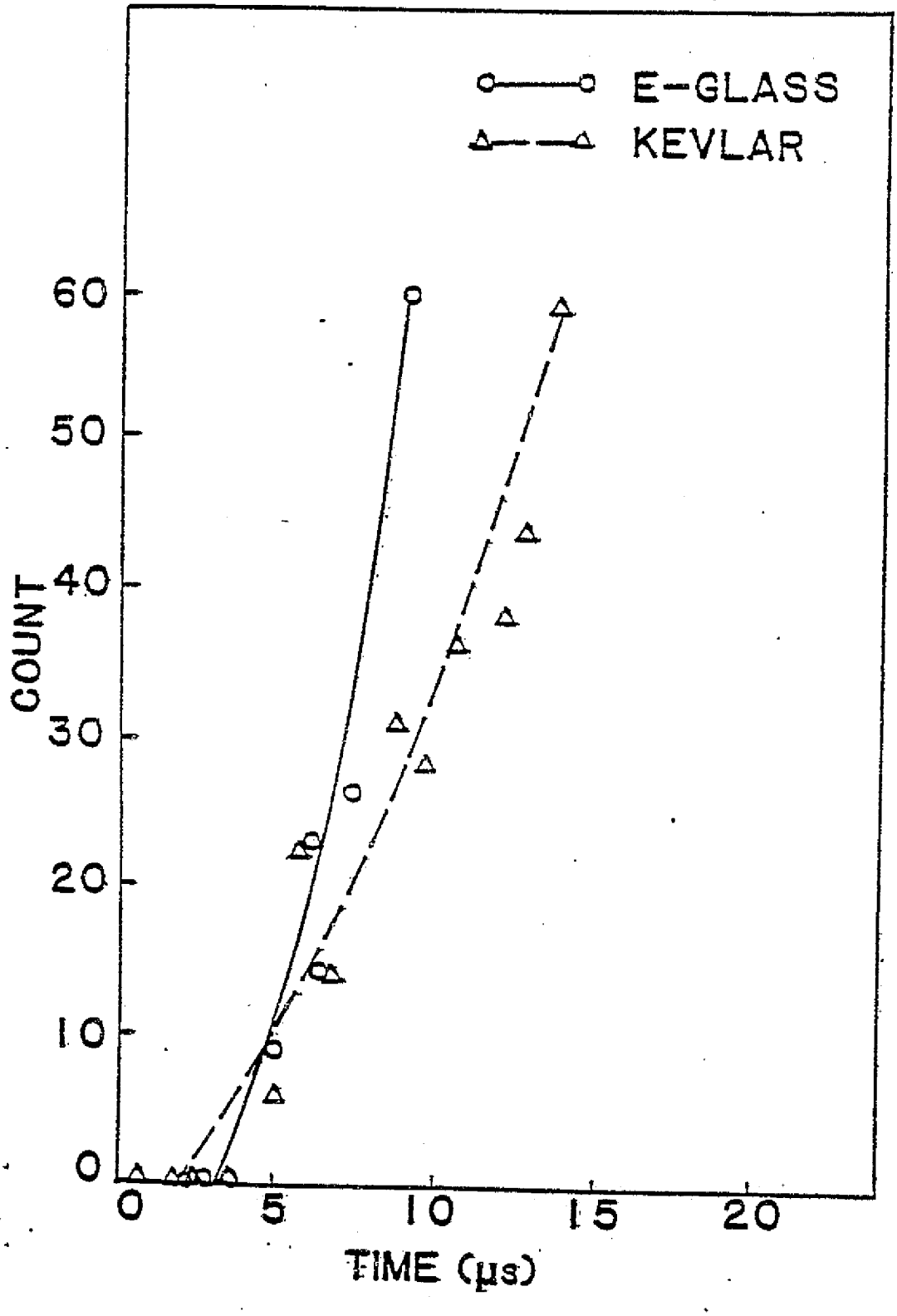

Fig. 8

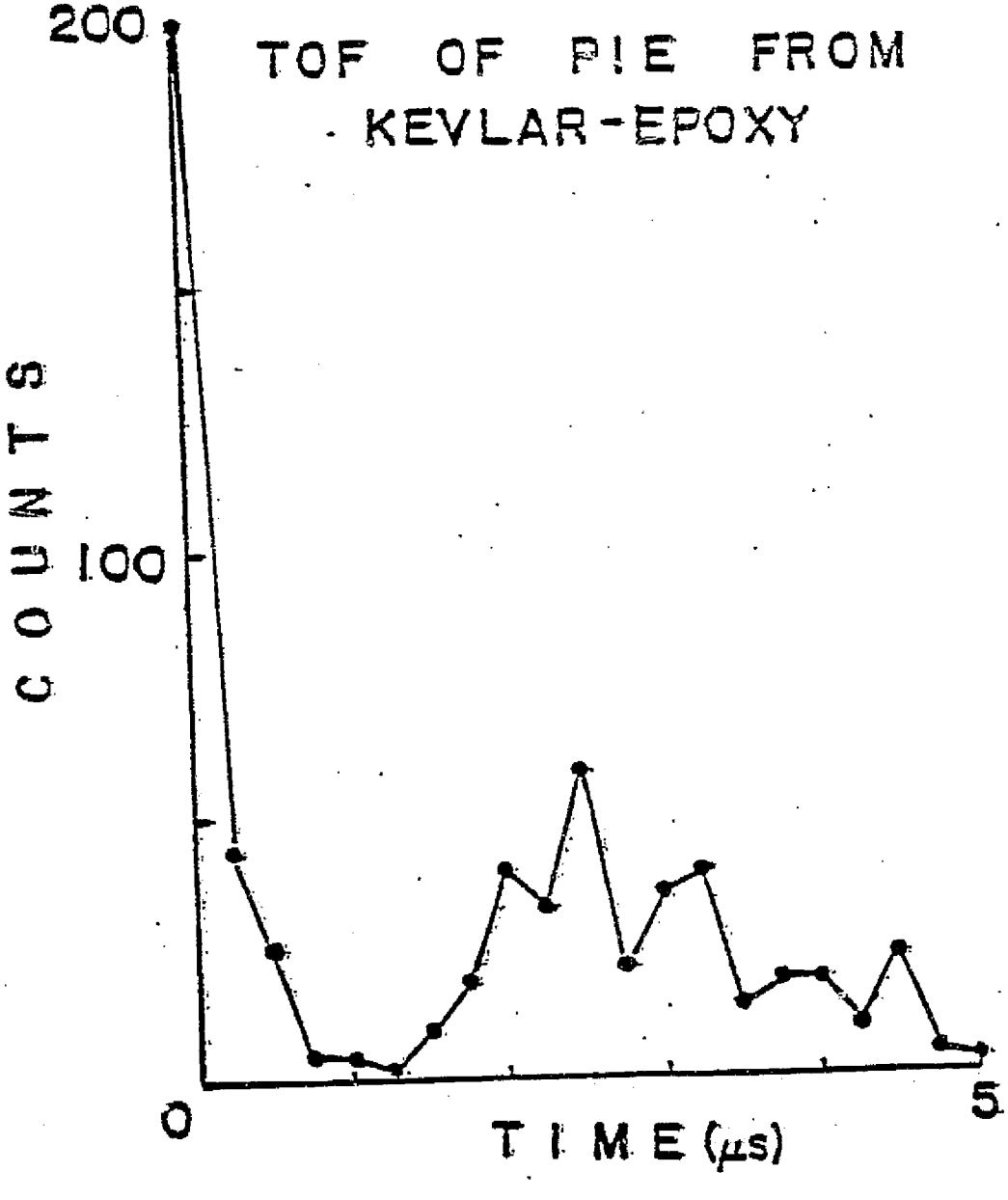

Fig. 9

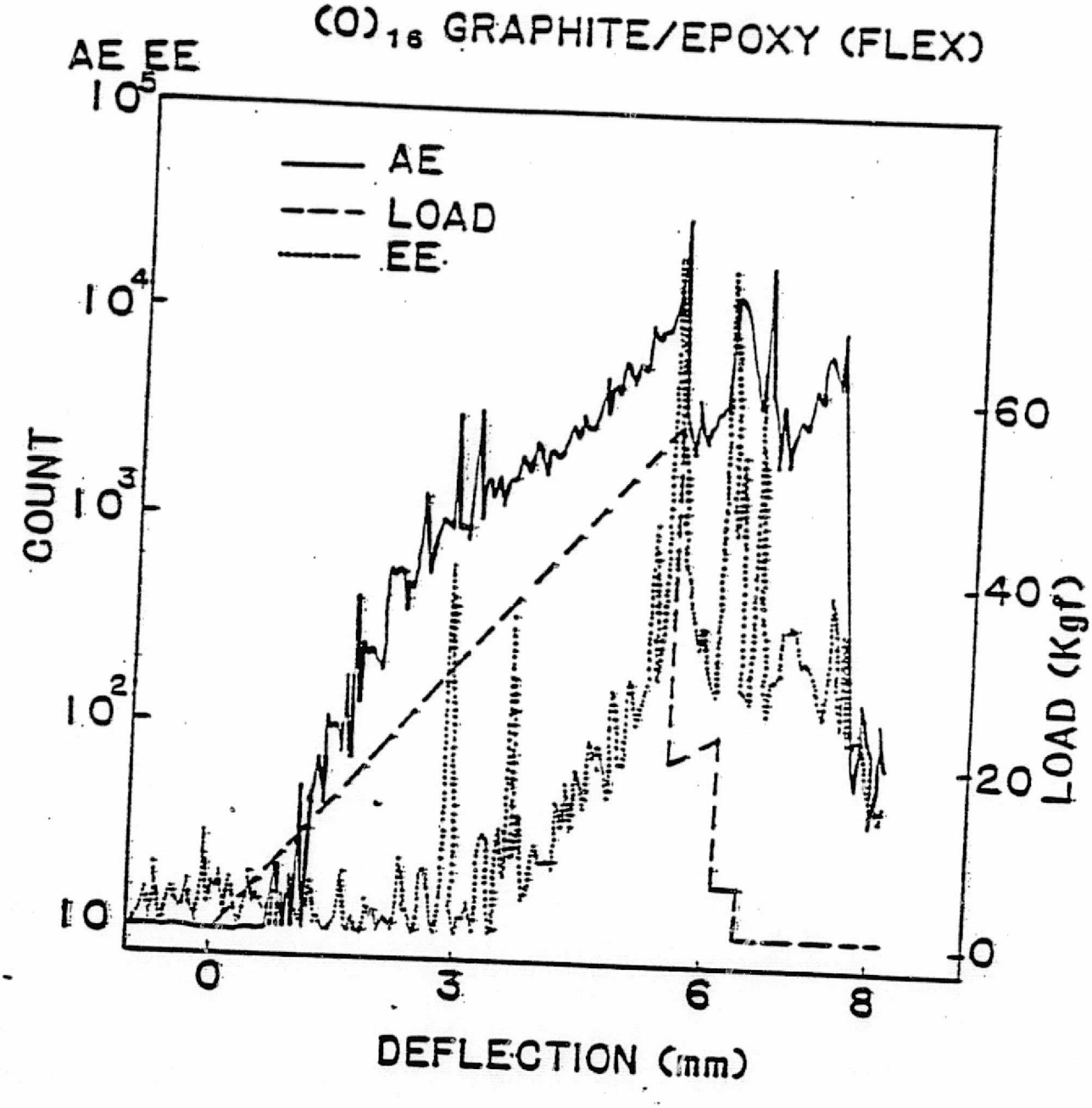

Fig. 10

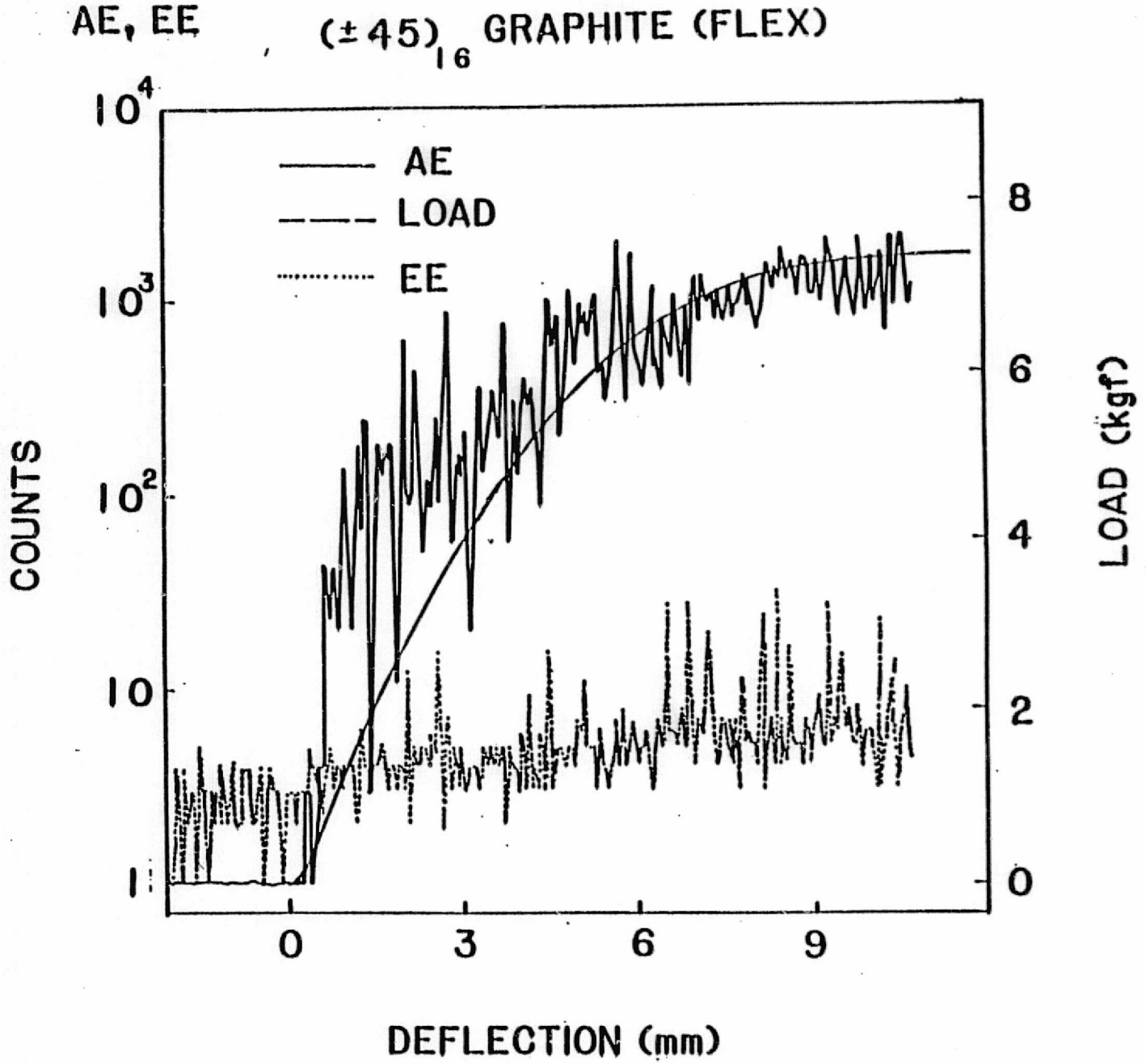

Fig. 11

ORIGINAL PAGE IS OF POOR QUALITY

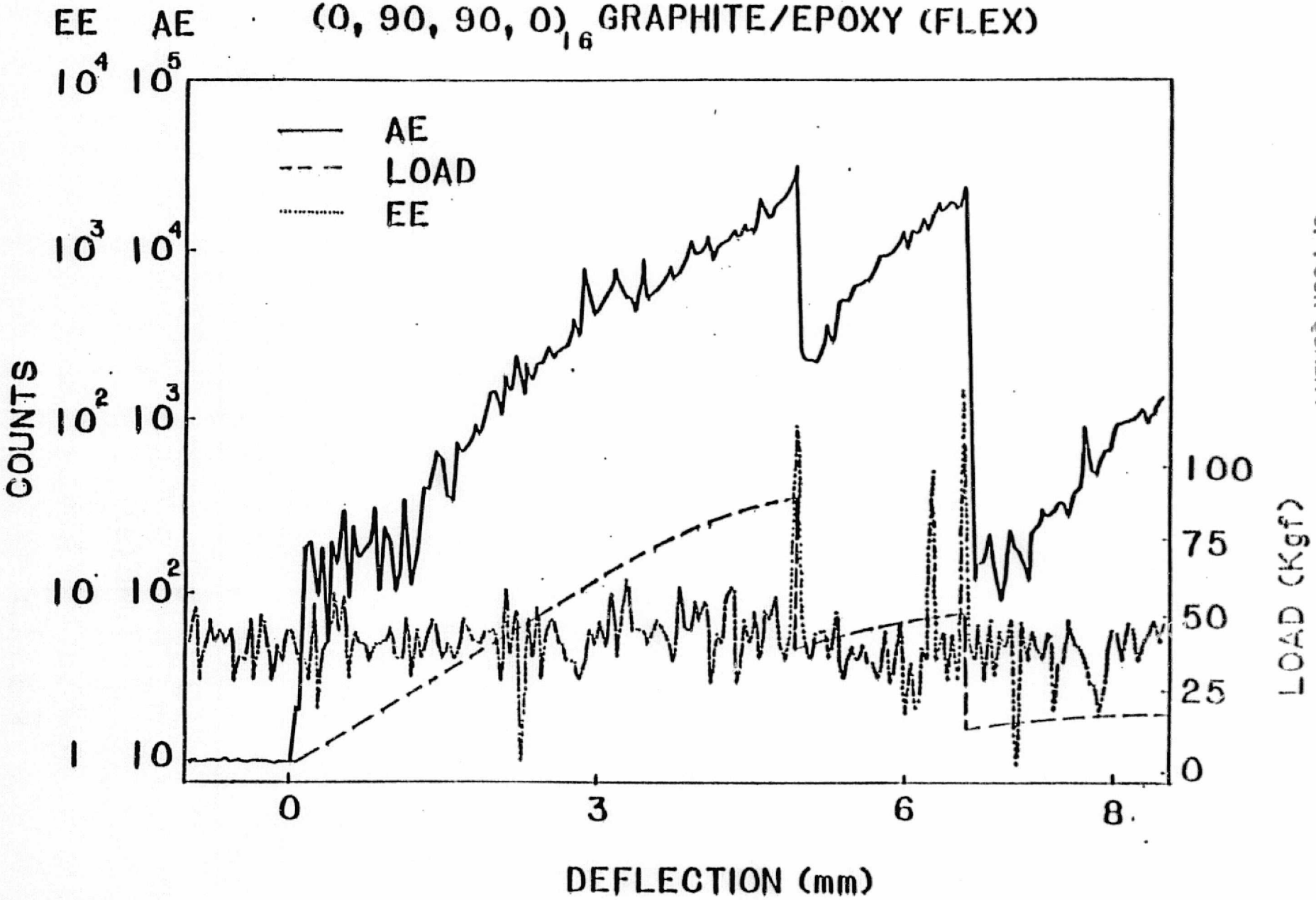

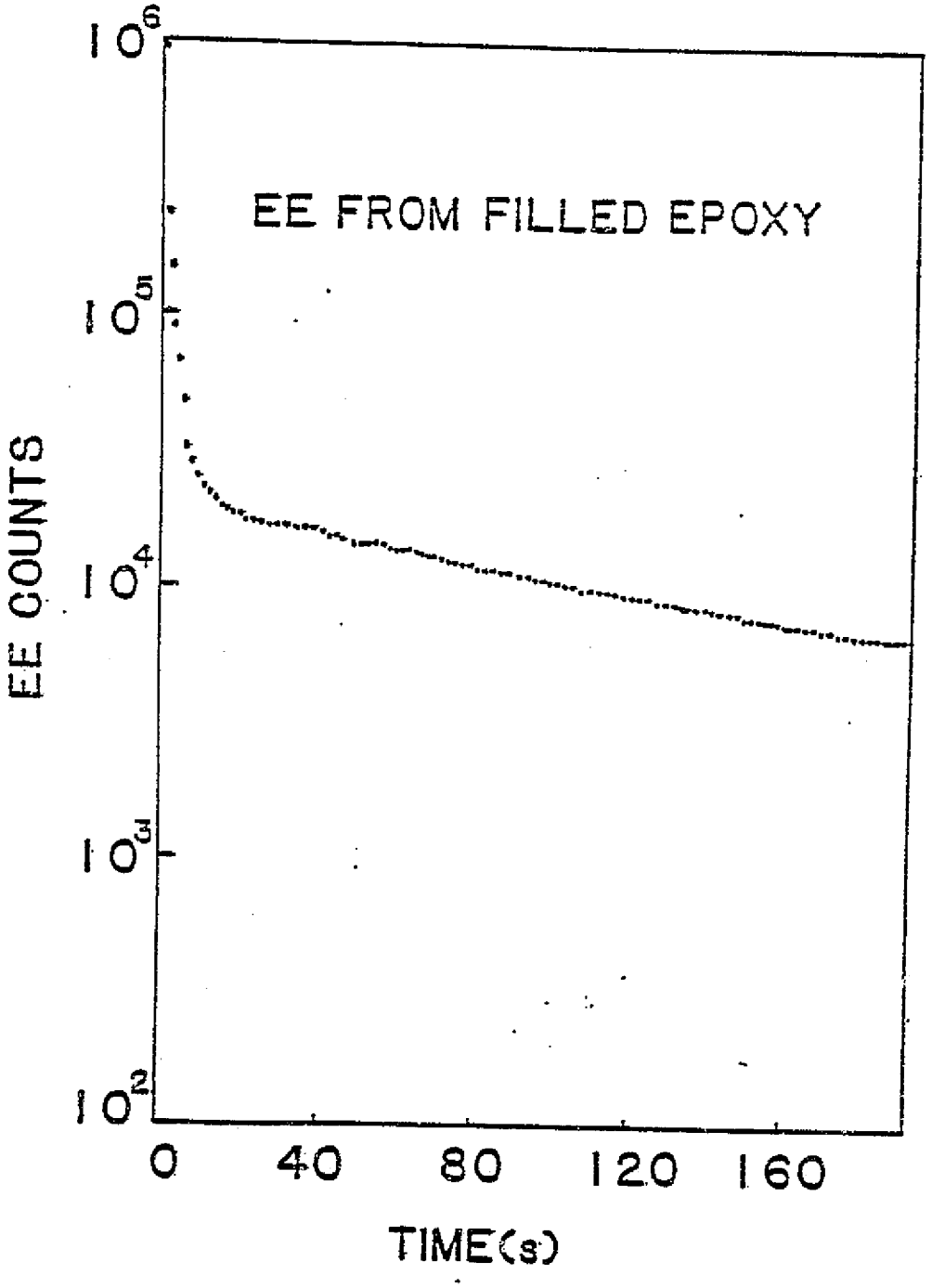

Fig. 13

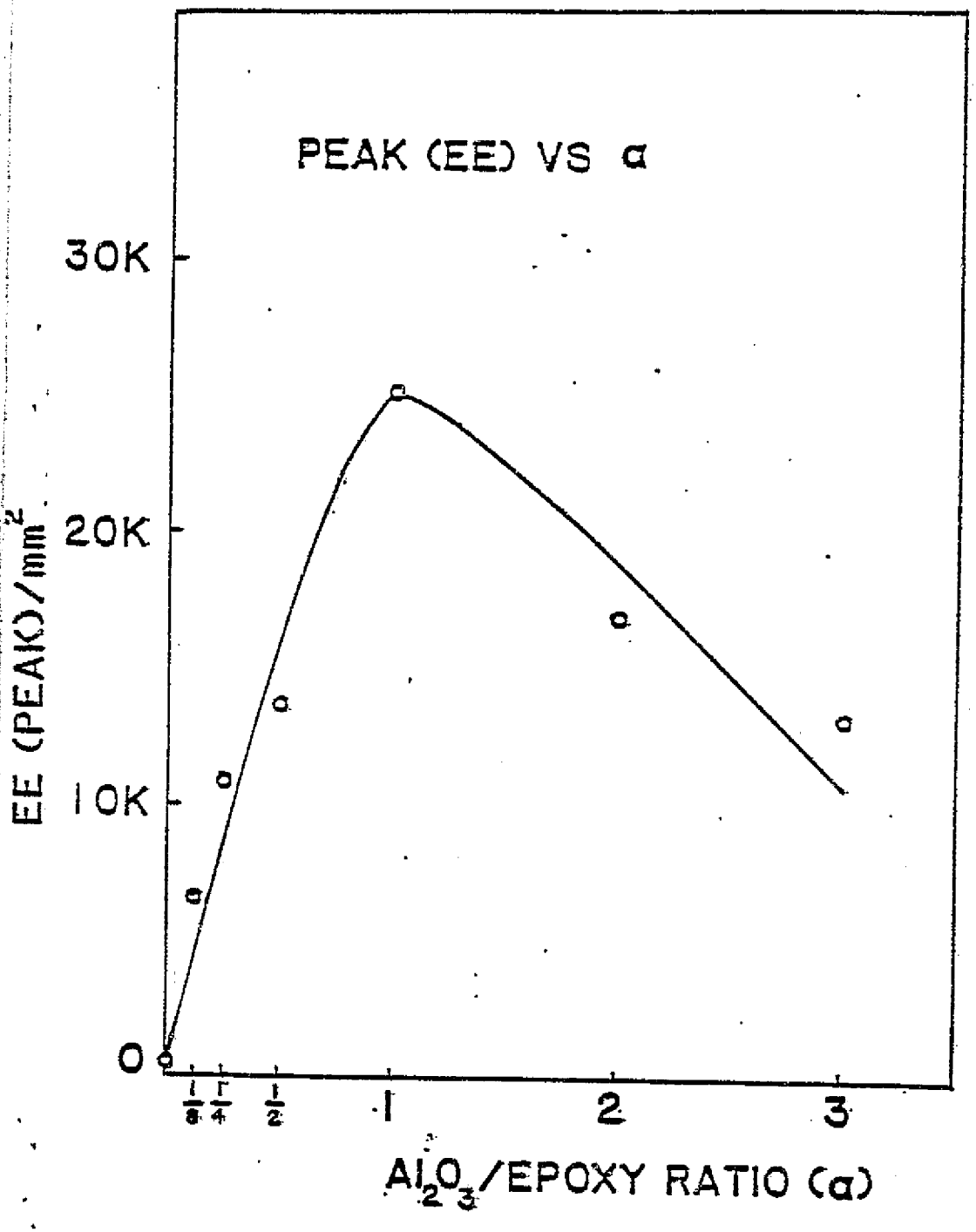

Fig. 14

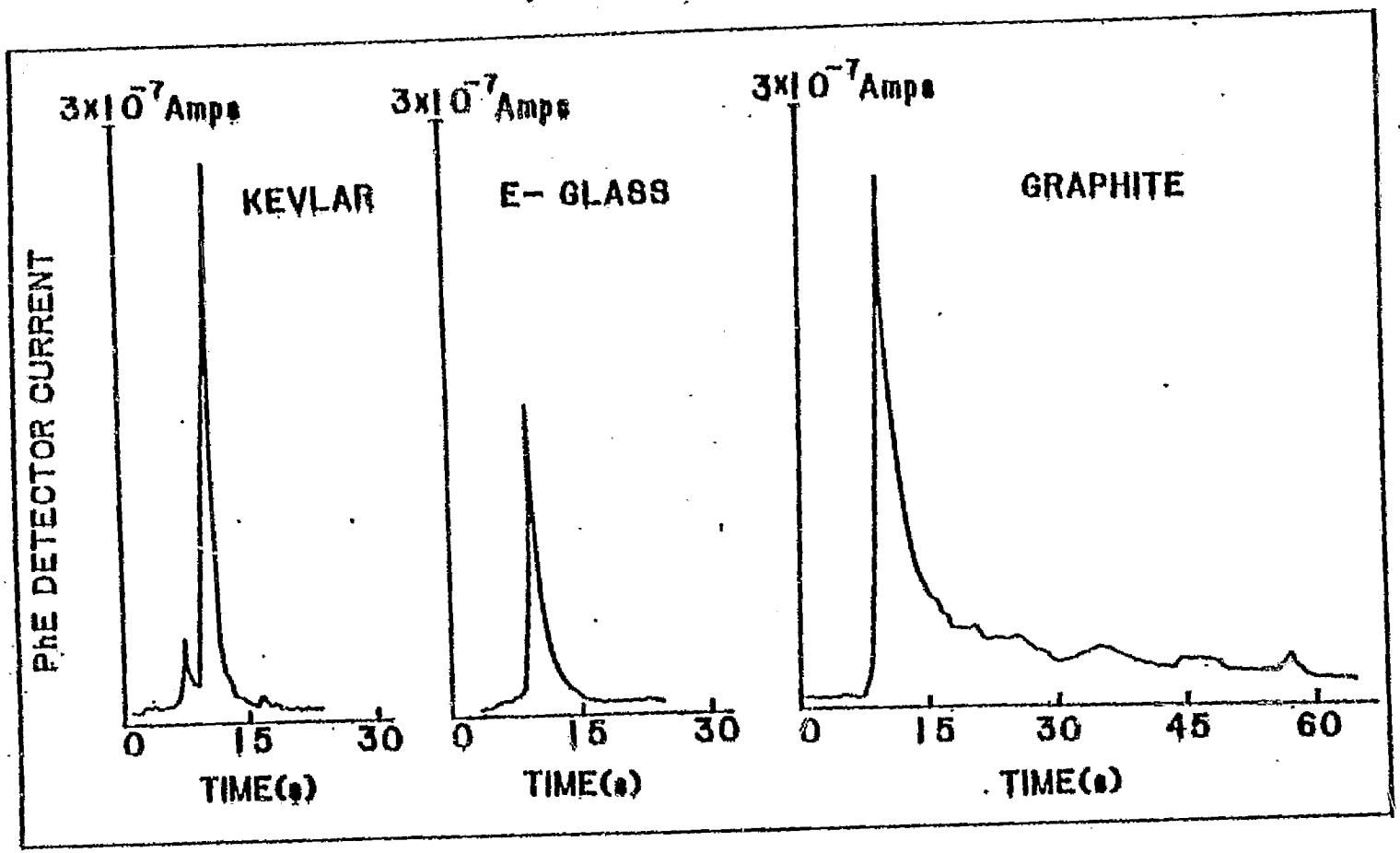

Fig. 15

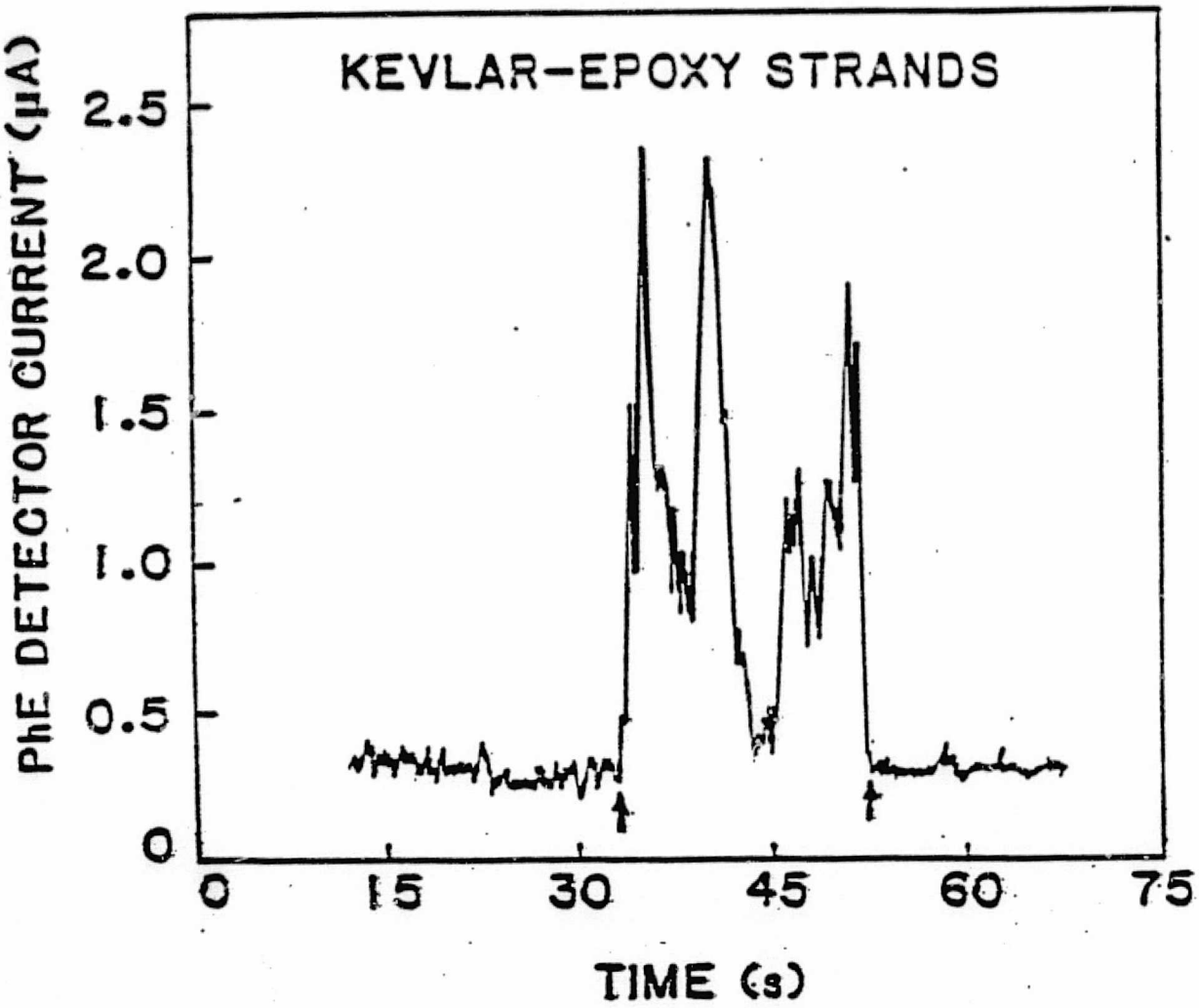

Fig. 16

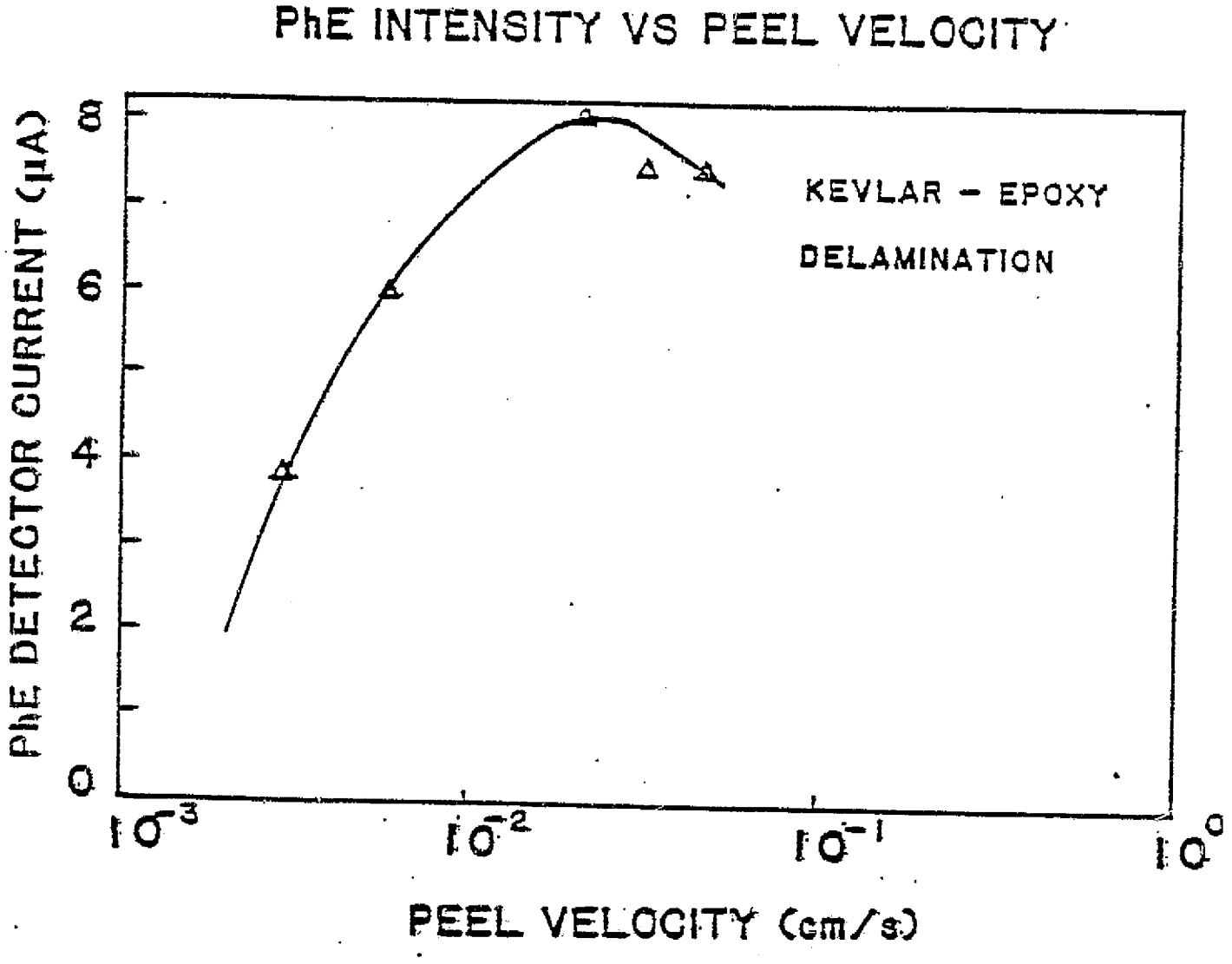

Fig. 17

VII. CONCLUSION

In this report we have presented our recent work on fracto-emission accompanying fiber and fiber/epoxy composite fracture. We also included recent studies on the mechanism of charged particle emission. Our goals are to continue our studies on characterizing the various FE components (charged particles, neutrals, and photons), to investigate the physical mechanisms responsible for this emission, and to correlate FE properties with the phenomena of fracture which are of interest to materials science. Our efforts to date have given us encouragement that FE promises to be a useful tool for probing failure mechanisms and detecting crack growth in composite materials.

VIII. FRACTO-EMISSION TALKS AND PAPERS PRESENTED

1. "Fracto-Emission from Elastomers," Gordon Conference on Elastomers, New Hampshire, July 1982.

2. "Correlations in Time of Electron and Positive Ion Emission Accompanying Fracture," American Vacuum Society, Baltimore, November 1982.

3. "Fracto-Emission from Composites," Gordon Conference on Composites, Santa Barbara, January 1983.

4. "Fracto-Emission Accompanying Adhesive Failure," ACS Symposium on Adhesion, Seattle, March 1983.

5. "Fracto-Emission from Fiber-Reinforced Composites and Adhesive Failure," ACS Symposium on Composites, Seattle, March 1983.

6. "Fracto-Emission from Filled and Unfilled Elastomers," ACS Symposium on Frontiers of Rubber Science, Toronto, May 1983.

7. "Fracto-Emission," DOW Chemical Company, Midland, MI, May 1983.